

# Credal Concept Bottleneck Models: Structural Separation of Epistemic and Aleatoric Uncertainty

Tanmoy Mukherjee<sup>1</sup> Marius Kloft<sup>2</sup> Pierre Marquis<sup>1</sup> Zied Bouraoui<sup>1</sup>

## Abstract

Decomposing predictive uncertainty into epistemic (model ignorance) and aleatoric (data ambiguity) components is central to reliable decision making, yet most methods estimate both from the same predictive distribution. Recent empirical and theoretical results show these estimates are typically strongly correlated, so changes in predictive spread simultaneously affect both components and blur their semantics. We propose a credal-set formulation in which uncertainty is represented as a *set* of predictive distributions, so that epistemic and aleatoric uncertainty correspond to distinct geometric properties: the size of the set versus the noise within its elements. We instantiate this idea in a Variational Credal Concept Bottleneck Model with two disjoint uncertainty heads trained by disjoint objectives and non-overlapping gradient paths, yielding separation by construction rather than post hoc decomposition. Across multi-annotator benchmarks, our approach reduces the correlation between epistemic and aleatoric uncertainty by over an order of magnitude compared to standard methods, while improving the alignment of epistemic uncertainty with prediction error and aleatoric uncertainty with ground-truth ambiguity.

## 1. Introduction

A medical AI that reports “70% confidence” offers limited guidance: should the clinician trust the prediction, order more tests, or request expert review? The answer depends on *why* the model is uncertain. Predictive uncertainty is commonly decomposed into epistemic uncertainty (EU, model ignorance) and aleatoric uncertainty (AU, data ambiguity). Crucially, these components support qualitatively different actions: EU should decrease as the model acquires more rel-

<sup>1</sup>CRIL UMR 8188, Univ Artois, CNRS, France <sup>2</sup>RPTU Kaiserslautern-Landau. Correspondence to: Tanmoy Mukherjee <mukherjee@cril.fr>.

Preprint. February 13, 2026.

evant evidence (e.g., more data or better coverage), whereas AU reflects persistent ambiguity and motivates abstention, human oversight, or communicating multiple plausible outcomes. In high-stakes settings, acting on the *type* of uncertainty can matter more than the overall magnitude.

Standard methods derive both uncertainties from the model’s predicted probabilities, creating an algebraic trap: when predictions are uncertain, both EU and AU increase together, producing strong correlation that blurs their distinct meanings. Recent evidence shows this coupling leads to an *empirical collapse*: across many uncertainty methods, epistemic and aleatoric estimates share most of their variance and are often strongly correlated (Mucsányi et al., 2024). Thus, methods that claim to decompose uncertainty often fail to separate these sources in practice. (Fig. 1a) From a complementary angle, Osband et al. (2022) shows that marginal predictions for single inputs are insufficient to distinguish uncertainty types and proposes Epistemic Neural Networks that introduce a dedicated epistemic component; however, AU remains implicit and unsupervised. This phenomenon is consistent with a formal limitation. Tomov et al. (2025) shows (in an idealized setting with access to the ground-truth label distribution  $p^*$ ) that one cannot recover both AU (e.g.,  $\mathbb{H}[p^*]$ ) and an error-related epistemic term from the model’s marginal prediction  $p(y | x)$  alone when multiple labels are valid. Intuitively, the same predictive spread can arise either from a confused model on a clear case or from a well-calibrated model facing genuine ambiguity (Fig. 1a). Relatedly, Osband et al. (2022) argues that marginal predictions are insufficient to isolate epistemic uncertainty and introduces Epistemic Neural Networks, though AU remains implicit.

These results imply that meaningful decomposition must access information beyond the predictive distribution. We therefore propose *structural separation*, where epistemic and aleatoric uncertainty is computed from distinct parameters trained by distinct objectives. EU is regularized toward a prior and designed to shrink with data, whereas AU is explicitly supervised to match persistent annotator disagreement. When the gradient sources are disjoint, algebraic coupling through  $p(y|x)$  is avoided by construction.

We instantiate the proposed structural separation in a *Vari-*

*ational Credal Concept Bottleneck Model* where credal sets are parameterized as ellipsoids and regularized via the Hausdorff KL divergence—the supremum KL over the set—which admits closed-form gradients for scalable optimization. We build on Concept Bottleneck Models (CBMs) (Koh et al., 2020), which route predictions through human-interpretable concepts and often provide multi-annotator concept labels. The resulting disagreement distributions act as direct supervision for aleatoric uncertainty. Our architecture uses three heads on a shared encoder: a task head, an epistemic head that parameterizes a credal covariance  $\Sigma_{\text{epi}}$  trained only via KL regularization, and an aleatoric head that predicts  $\sigma_{\text{ale}}^2$  trained only on annotator disagreement. Instead of point concept predictions, we represent each concept as a *credal set* (an ellipsoidal region of plausible distributions):  $\Sigma_{\text{epi}}$  sets the region size (epistemic), and  $\sigma_{\text{ale}}^2$  captures ambiguity within the region (aleatoric). We derive a Credal ELBO in which these components receive gradients from disjoint loss terms. Our contributions are:

1. We connect the empirical collapse of standard decompositions (Mucsányi et al., 2024) to the impossibility of recovering (EU, AU) from predictive distributions alone (Tomov et al., 2025).
2. We identify structural separation (disjoint parameterization and disjoint gradients) as a escape principle.
3. We introduce Variational Credal CBMs with a Credal ELBO that induces structural separation by design.
4. On CEBaB, HateXplain, and GoEmotions, we observe that EU and AU are nearly uncorrelated, in contrast to the strong correlations seen for baseline methods, with EU tracking prediction error and AU reflecting annotator disagreement, which in turn supports more effective active learning and concept-level interventions.

## 2. Background

We establish notation, formalize epistemic and aleatoric uncertainty, explain why standard decompositions fail, and motivate structural separation.

**Notation** We denote inputs as  $x \in \mathcal{X}$ , task labels as  $y \in \{1, \dots, J\}$ , and concept labels as  $c \in \{1, \dots, K\}^C$  for  $C$  concepts with  $K$  classes each (e.g.,  $K = 3$  for negative/unknown/positive). The encoder produces representations  $h = f_{\text{enc}}(x) \in \mathbb{R}^d$ . We write  $\Delta^{K-1}$  for the  $(K-1)$ -simplex of probability distributions. A key distinction:  $p(c|x)$  denotes the model’s predicted distribution over concepts, while  $p^*(c|x)$  denotes the true (unknown) distribution reflecting genuine label ambiguity—when multiple annotators disagree,  $p^*$  has high entropy. For uncertainty,  $U_{\text{epi}}$  denotes epistemic uncertainty (model ignorance about  $p^*$ ) and  $U_{\text{ale}}$  denotes aleatoric uncertainty (entropy of  $p^*$

itself). The credal set  $\mathcal{C} \subset \Delta^{K-1}$  is parameterized by mean  $\mu \in \mathbb{R}^K$ , epistemic covariance  $\Sigma_{\text{epi}} \in \mathbb{R}_{++}^{K \times K}$ , and aleatoric variance  $\sigma_{\text{ale}}^2 \in \mathbb{R}_+$ . We use  $\rho(\cdot, \cdot)$  for Spearman correlation. Complete notation is in Appendix A.

## 2.1. Uncertainty Decomposition

Predictive uncertainty has distinct sources that demand different responses. For an input  $x$ , we distinguish: **Epistemic uncertainty (EU)**, due to limited data or model capacity, which is *reducible* with more data or better models; and **Aleatoric uncertainty (AU)**, due to inherent data ambiguity, which is *irreducible* even for an optimal model with infinite data. For example, annotators may legitimately disagree on whether “interesting food” is positive or neutral. Following Tomov et al. (2025), let  $p^*$  denote the ground-truth distribution induced by infinitely many competent annotators, and let  $p$  be the model prediction. We define

$$\text{EU}(x) = D_{\text{KL}}(p^* \parallel p), \quad \text{AU}(x) = H[p^*]. \quad (1)$$

EU measures divergence from the truth, whereas AU measures intrinsic ambiguity of the truth itself. The distinction is operational: high EU motivates further learning, high AU motivates human review.

## 2.2. Why decomposition from $p$ alone can fail

Standard approaches derive both EU and AU from the same object: the model’s marginal predictive probabilities at  $x$  (or statistics of sampled predictors such as dropout/ensembles). Typically, AU is estimated by prediction entropy, while EU is estimated by variability across model samples (e.g., mutual information). Because both are functions of the same predictive probabilities, the two estimates can become strongly coupled in practice (Mucsányi et al., 2024). Tomov et al. (2025) formalize a limitation underlying this coupling: when multiple labels are valid, marginal predictions alone do not uniquely determine whether predictive spread stems from model error or intrinsic ambiguity. Intuitively, the same prediction  $p(\cdot|x)$  may arise from (i) a confused model on a clear case (high EU, low AU) or (ii) a calibrated model on an ambiguous case (low EU, high AU), making post hoc decomposition from  $p$  ill-posed (Fig. 1).

**Prior Architectures and Limitations** Heteroscedastic models (Kendall and Gal, 2017) add a separate output head for aleatoric uncertainty, but epistemic uncertainty is still obtained from Monte Carlo Dropout variance over the predicted probabilities. Epistemic Neural Networks (Osband et al., 2022) separate epistemic uncertainty via an additional epinet, but aleatoric uncertainty is only implicit—defined as whatever does not change with the epistemic index, without explicit supervision. Neither method achieves a complete separation of the two types of uncertainty.

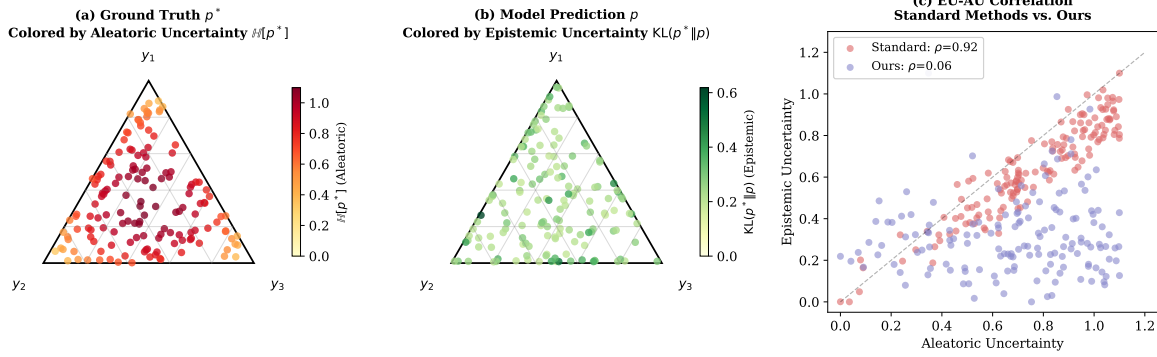


**Figure 1. Why standard decomposition fails.** Aleatoric uncertainty reflects where  $p^*$  lies on the simplex—ambiguous cases cluster near the center (**left**). Epistemic uncertainty reflects how far  $p$  deviates from  $p^*$  (**middle**). These are geometrically independent properties, yet methods deriving both from  $p$  produce estimates that fall along a diagonal (**right, red**)—the “algebraic trap.” Credal CBM’s structural separation recovers the independence (**right, blue**).

**Table 1.** Comparison of uncertainty decomposition approaches. Only structural separation explicitly parameterizes and supervises both uncertainty types.

|                | Ensemble                    | Kendall       | ENN      | Ours                       |
|----------------|-----------------------------|---------------|----------|----------------------------|
| AU source      | $\mathbb{E}[\mathbb{H}[p]]$ | $\sigma^2(x)$ | Implicit | $\sigma_{\text{ale}}$ head |
| EU source      | Var of $p$                  | MC Dropout    | Epinet   | $\Sigma_{\text{epi}}$ head |
| EU from $p^*$  | Yes                         | Yes           | No       | <b>No</b>                  |
| AU supervised? | No                          | Implicit      | No       | <b>Yes</b>                 |

### 2.3. Structural Separation

To avoid ill-posed post hoc decomposition, we propose *structural separation*: EU and AU are computed from disjoint parameters and trained from disjoint learning signals.

**Definition 2.1** (Structural Separation). *A model satisfies structural separation if: (i) EU and AU are parameterized by disjoint variables  $\phi_{\text{epi}}$  and  $\phi_{\text{ale}}$ ; (ii) their learning signals have disjoint gradient sources; and (iii) each is supervised consistent with its semantics.*

**Why Concept Bottleneck Models?** CBMs provide the missing supervision signal. Their multi-annotator concept labels yield disagreement distributions estimating  $p^*$ , directly supervising AU. If three of five annotators label a concept AS POSITIVE and two AS UNKNOWN, then  $\hat{p}^* = (0, 0.6, 0.4)$  with  $\mathbb{H}[\hat{p}^*] = 0.67$ —this supervises  $\sigma_{\text{ale}}$ . Table 1 contrasts structural separation with prior approaches.

## 3. Method: Credal Concept Bottleneck Models

Section 2 established that decomposition fails when both uncertainties derive from the same predictive distribution  $p(y|x)$ . We present Credal CBMs, which represent uncertainty as a *credal set* where epistemic and aleatoric components arise from geometrically distinct elements trained by disjoint objectives.

### 3.1. Credal Set Representation

We parameterize credal sets as ellipsoids in logit space. For input  $x$  with  $K$  outcomes:

$$\mathcal{C}(x) = \left\{ \text{softmax}(z) : (z - \mu)^\top \Sigma_{\text{epi}}^{-1} (z - \mu) \leq 1 \right\} \quad (2)$$

where  $\mu \in \mathbb{R}^K$  is the credal center and  $\Sigma_{\text{epi}} = \text{diag}(\sigma_{\text{epi},1}^2, \dots, \sigma_{\text{epi},K}^2)$  is the shape matrix. Each uncertainty type occupies a geometrically distinct role:

$$\text{Epistemic: } U_{\text{epi}} = \log \det(\Sigma_{\text{epi}}) = \sum_{k=1}^K \log \sigma_{\text{epi},k}^2 \quad (3)$$

$$\text{Aleatoric: } U_{\text{ale}} = \sigma_{\text{ale}} \quad (4)$$

### 3.2. Architecture and Training

Our architecture (Fig. 2) instantiates structural separation through a frozen encoder and three *orthogonally projected* heads. Given input  $x$ , the encoder produces  $h = f_{\text{enc}}(x) \in \mathbb{R}^d$ . An orthogonal projection maps  $h$  into disjoint subspaces:

$$h_\mu = W_\mu h, \quad h_{\text{epi}} = W_{\text{epi}} h, \quad h_{\text{ale}} = W_{\text{ale}} h \quad (5)$$

where  $W_\mu, W_{\text{epi}}, W_{\text{ale}} \in \mathbb{R}^{d/2 \times d}$  are orthogonally initialized and regularized via  $\mathcal{L}_{\text{orth}} = \|W_{\text{epi}}^\top W_{\text{ale}}\|_F^2$ . Each subspace feeds a dedicated head:

$$\mu = g_\mu(h_\mu; \phi_\mu) \quad (\text{credal center}) \quad (6)$$

$$\sigma_{\text{epi}} = \text{softplus}(g_{\text{epi}}(h_{\text{epi}}; \phi_{\text{epi}})) \quad (\text{credal size}) \quad (7)$$

$$\sigma_{\text{ale}} = \text{softplus}(g_{\text{ale}}(h_{\text{ale}}; \phi_{\text{ale}})) \quad (\text{aleatoric head}) \quad (8)$$

**Aleatoric Loss.** The aleatoric head predicts annotator disagreement entropy:

$$\mathcal{L}_{\text{ale}} = \frac{1}{C} \sum_{c=1}^C \left( \sigma_{\text{ale}}^{(c)} - \mathbb{H}[\hat{p}^{*(c)}] \right)^2 \quad (9)$$

where  $\mathbb{H}[\hat{p}^{*(c)}]$  is the empirical annotator entropy for concept  $c$ , used as supervision target only (not as input to  $g_{\text{ale}}$ ).

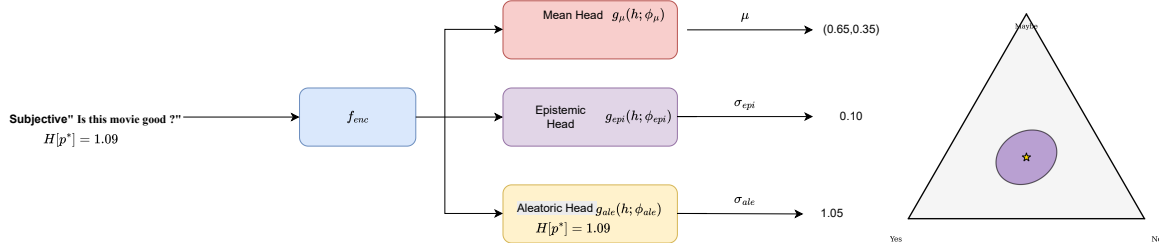


**Figure 2. Credal CBM architecture.** For “Is this movie good?” ( $H[p^*] = 1.09$ ), the credal set lies in the simplex interior and  $\sigma_{\text{ale}} = 1.05$  reflects annotator disagreement. For factual questions like “What is 2+2?” ( $H[p^*] = 0.12$ ), the credal set would be near a vertex with  $\sigma_{\text{ale}} = 0.15$ .

**Epistemic Loss.** The epistemic head combines error supervision with Hausdorff KL regularization:

$$\mathcal{L}_{\text{epi}} = \underbrace{\frac{1}{C} \sum_{c=1}^C \left( \sigma_{\text{epi}}^{(c)} - \phi(|\hat{p}^{(c)} - c^{(c)}|_{\text{sg}}) \right)^2}_{\text{error supervision}} + \underbrace{\beta \cdot D_H^+(\mathcal{C} \parallel \mathcal{C}_{\text{prior}})}_{\text{Hausdorff KL}} \quad (10)$$

where  $\hat{p}^{(c)} = \sigma(\mu^{(c)})$  is the predicted concept probability,  $c^{(c)} \in \{0, 1\}$  is the ground-truth label,  $|\cdot|_{\text{sg}}$  denotes stop-gradient (`detach()`), and  $\phi(e) = \alpha e + \sigma_{\min}$  scales errors to  $[\sigma_{\min}, \sigma_{\max}]$ .

**Error supervision** makes  $\sigma_{\text{epi}}$  input-dependent: high-error concepts receive large credal sets. The stop-gradient prevents the head from “gaming” the loss.

**Hausdorff KL**  $D_H^+ = \sup_{q \in \mathcal{C}} D_{\text{KL}}(q \parallel p_0)$  regularizes credal set volume toward a prior. For diagonal  $\Sigma_{\text{epi}}$  and isotropic prior, this admits closed form with  $O(K)$  complexity (Appendix D, Proposition D.1).

### Full Objective.

$$\mathcal{L} = \mathcal{L}_{\text{task}} + \lambda_c \mathcal{L}_{\text{concept}} + \lambda_e \mathcal{L}_{\text{epi}} + \lambda_a \mathcal{L}_{\text{ale}} + \lambda_o \mathcal{L}_{\text{orth}} \quad (11)$$

Details on training and inference are provided in Appendix B.

### 3.3. Why Gradient Separation Matters

The infeasibility of Tomov et al. (2025) shows that deriving both uncertainties from  $p$  produces correlation. But *why* does our architecture escape this? Without gradient isolation, any shared gradient path—through the encoder, cross-coupled losses, or joint supervision—means updates that improve one head also affect the other. Even with separate parameters, optimization dynamics still correlate their uncertainties. The frozen encoder prevents gradient coupling between heads. Updates to  $\phi_{\text{epi}}$  through  $\mathcal{L}_{\text{epi}}$  and  $D_H^+$  cannot affect  $\phi_{\text{ale}}$ , and vice versa. Updates to  $\phi_{\text{epi}}$  through  $\mathcal{L}_{\text{epi}}$  and  $D_H^+$  cannot affect  $\phi_{\text{ale}}$ , and vice versa.  $\phi_{\text{epi}}$  receives gradients only from epistemic losses ( $\mathcal{L}_{\text{epi}}$  and  $D_H^+$ ),  $\phi_{\text{ale}}$  only from the aleatoric loss ( $\mathcal{L}_{\text{ale}}$ ), and the frozen encoder

prevents any gradient coupling. This is not mere regularization but a *structural guarantee* that the two heads cannot influence each other during learning. We formalize this:

### 3.4. Theoretical Guarantees

**Theorem 3.1** (Gradient Separation). *Let  $\mathcal{L} = \mathcal{L}_{\text{task}} + \lambda_c \mathcal{L}_{\text{concept}} + \lambda_e \mathcal{L}_{\text{epi}} + \lambda_a \mathcal{L}_{\text{ale}} + \lambda_o \mathcal{L}_{\text{orth}}$  with frozen encoder, orthogonal projections, and stop-gradient in  $\mathcal{L}_{\text{epi}}$  (Eq. 10). Then:*

$$\nabla_{\phi_{\text{ale}}} \mathcal{L} = \lambda_a \nabla_{\phi_{\text{ale}}} \mathcal{L}_{\text{ale}} \quad (12)$$

$$\nabla_{\phi_{\text{epi}}} \mathcal{L} = \lambda_e \nabla_{\phi_{\text{epi}}} \mathcal{L}_{\text{epi}} \quad (13)$$

*That is, aleatoric parameters receive gradients only from  $\mathcal{L}_{\text{ale}}$ , while epistemic parameters receive them from  $\mathcal{L}_{\text{epi}}$ .*

*Proof.* See Appendix E.1.  $\square$

**Remark 3.2** (Optional Decorrelation Penalty). *One may add an explicit decorrelation term  $\mathcal{L}_{\text{decorr}} = \rho(\sigma_{\text{epi}}, \sigma_{\text{ale}})^2$  to the objective. This intentionally couples the heads via a shared gradient signal that encourages decorrelation. In our experiments, structural separation alone achieves  $|\rho| < 0.1$ , so we set  $\lambda_d = 0$  by default. The decorrelation penalty provides marginal additional benefit (Table 3) and may be useful when orthogonal projection is disabled.*

<sup>1</sup>

**Corollary 3.3** (Asymptotic Decorrelation). *Under Theorem 3.1, if:*

- (i)  $\mathcal{L}_{\text{epi}}$  and  $\mathcal{L}_{\text{ale}}$  converge to small values,
- (ii) their supervision targets (prediction errors and annotator entropy) are approximately uncorrelated in the data distribution,
- (iii) the orthogonal projections extract sufficiently distinct features,

<sup>1</sup> Gradient separation is a necessary condition for decorrelation—without it, optimizing  $\mathcal{L}_{\text{ale}}$  would inadvertently influence  $\sigma_{\text{epi}}$ . However, gradient separation alone does not guarantee output independence, since both heads map from the same  $h$ . Decorrelation additionally requires that supervision targets are uncorrelated.

then  $\rho(\sigma_{\text{epi}}, \sigma_{\text{ale}}) \rightarrow 0$  as training converges.

*Proof Sketch.* At convergence with sufficient capacity,  $\sigma_{\text{epi}}(x) \approx \phi(\text{err}(x))$  and  $\sigma_{\text{ale}}(x) \approx \mathbb{H}[\hat{p}^*(x)]$ . By condition (ii),  $\text{Cov}(\text{err}, \mathbb{H}) \approx 0$  in the data. Gradient separation (Theorem 3.1) ensures that each head optimizes only its own target without interference. Condition (iii) prevents the heads from extracting identical features that would reintroduce correlation.  $\square$

**Remark 3.4.** Condition (iii) is encouraged but not guaranteed by orthogonal projection—both heads still receive information from the same encoder output  $h$ .

**Empirical validation.** Fig 3 Decorrelation emerges quickly in early training and stabilizes confirming that structural separation enables decorrelation once heads learn meaningful representations. On MAQA\* with ground-truth supervision,  $\rho(\sigma_{\text{ale}}, \mathbb{H}[p^*]) = 0.78$ , showing AU tracks true ambiguity.

## 4. Experiments

We evaluate Variational Credal CBM through three research questions: **(RQ1)** Does structural separation achieve decorrelation ( $\rho(U_{\text{epi}}, U_{\text{ale}}) \rightarrow 0$ )? **(RQ2)** Does each uncertainty track its intended target (errors vs. ambiguity)? **(RQ3)** Does the method escape collapse under high ambiguity?

### 4.1. Experimental Setup

**Datasets.** We evaluate four datasets : CEBaB and GoEmotions for classification with annotator disagreement, and MAQA\*/AmbigQA\* from Tomov et al. (2025), which provide **ground-truth** answer distributions  $p^*$  from factual co-occurrence—enabling gold-standard validation of  $U_{\text{ale}}$  against true ambiguity  $\mathbb{H}[p^*]$ . Details are in Appendix H.

**Implementation.** We use a frozen DistilBERT encoder with three lightweight heads for  $\mu$ ,  $\sigma_{\text{epi}}$ , and  $\sigma_{\text{ale}}$ . The encoder is frozen to ensure gradient isolation (Theorem 3.1). Training details and encoder ablations are located in Appendix K.

**Baselines.** We benchmark our approach against the methods from Tomov et al. (2025) that fail in the presence of ambiguity. Full implementation details are given in Appendix K.4.

### 4.2. Main Results

Table 2 summarizes performance across CeBAB and MAQA\*. Across all benchmarks, standard uncertainty estimators exhibit strong coupling between epistemic and aleatoric scores, whereas Credal CBM produces near-zero  $\rho(U_{\text{epi}}, U_{\text{ale}})$  while improving the semantic validity of both signals. This is consistent with the limitation that EU/AU cannot be uniquely disentangled from marginal predictive probabilities alone: Credal CBM circumvents these conditions by using disjoint parameterizations and disjoint learn-

ing signals. Full results on HateXplain, GoEmotions, and AmbigQA\* in Appendix J Table 11.

**RQ1: Decorrelation.** Table 2 shows that standard methods exhibit strong correlation between epistemic and aleatoric uncertainty, confirming the algebraic trap. Credal set methods (CreINNs, CBDL) achieve only a modest reduction in this correlation through geometric representations and still show substantial dependence. In contrast, Variational Credal CBM reduces the correlation to a negligible level—an order-of-magnitude improvement that validates Theorem 3.1: structural separation via gradient isolation enables empirical decorrelation where geometric representations alone cannot.

**RQ2: Validity against ground truth.** Beyond decorrelation, each uncertainty must track its intended target. We validate epistemic uncertainty against prediction errors ( $\rho(\mathcal{U}_{\text{epi}}, \mathbb{1}[\hat{y} \neq y])$ ) and—critically—aleatoric uncertainty against ground-truth ambiguity ( $\rho(\mathcal{U}_{\text{ale}}, \mathbb{H}[p^*])$ ) on datasets with multi-annotator labels or factual co-occurrence statistics. Table 2 shows our proposed Credal CBM substantially improves aleatoric validity across MAQA\* and AmbigQA\* compared to other baselines. This is a validation where learned aleatoric uncertainty is evaluated directly against ground-truth ambiguity, rather than derived post hoc from the predictive distribution used for epistemic uncertainty. The improvement shows that structural separation allows  $\mathcal{U}_{\text{ale}}$  to capture true ambiguity instead of model artifacts.

**RQ3: Robustness Under Ambiguity** When ground truth is ambiguous ( $\mathbb{H}[p^*] > 0$ ), EU and AU are not identifiable from marginal predictions alone (Tomov et al., 2025), which empirically yields worse error detection as ambiguity increases. We stratify MAQA\* by ambiguity into Low ( $\mathbb{H}[p^*] < 0.5$ ), Medium ( $0.5 \leq \mathbb{H}[p^*] < 1.5$ ), and High ( $\mathbb{H}[p^*] \geq 1.5$ ) quantile bins and measure AUROC for error detection in each. As ambiguity rises, baseline AUROC approaches chance, while Credal CBM degrades more slowly and stays consistently higher (Table 15).

### 4.3. Ablation Studies

We ablate key architectural components to validate our design choices and isolate the contribution of each element.

**Structural separation is necessary.** Tab. 3 shows that both a frozen encoder and disjoint heads are necessary for decorrelation. A trainable encoder couples gradients through backpropagation, and shared heads couple uncertainties through shared parameters. Only their combination yields negligible correlation, validating Theorem 3.1.

**Supervision ensures validity.** Removing aleatoric supervision ( $\lambda_{\text{ale}} = 0$ ) preserves decorrelation but harms validity:  $\rho(\mathcal{U}_{\text{ale}}, \mathbb{H})$  drops markedly. Thus, structural separation provides architectural decorrelation, but supervision is needed for semantic grounding. The decorrelation penalty gives

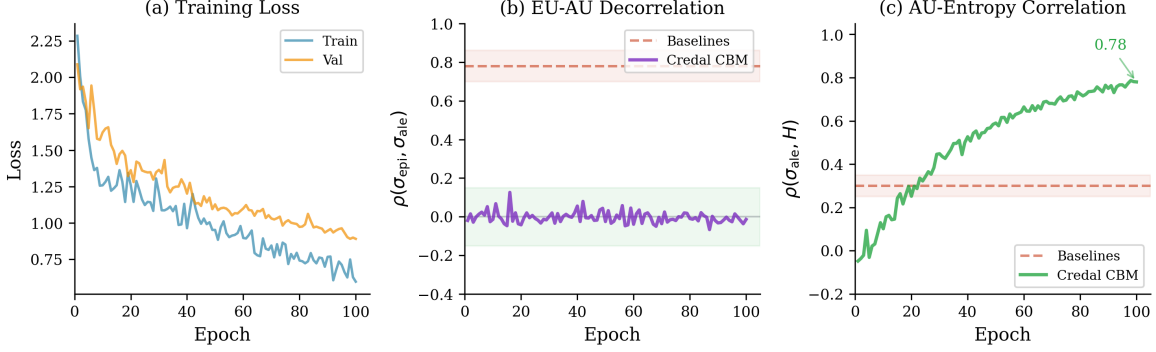


**Figure 3. Empirical validation of Theorem 3.1.** (a) Training loss convergence. (b) EU–AU correlation over training: baselines maintain strong coupling throughout (red,  $\rho > 0.7$ ), while Credal CBM achieves decorrelation within 10–20 epochs (blue/purple), stabilizing near  $\rho \approx 0$ . The rapid initial drop reflects structural separation taking effect once heads begin learning. (c) AU–Entropy correlation: with ground-truth supervision on MAQA\*, aleatoric uncertainty tracks annotator entropy ( $\rho = 0.78$ ), while EU–AU decorrelation is preserved.

**Table 2. Main results with ambiguity stratification.** Variational Credal CBM achieves low correlation and maintains robustness under ambiguity. MAQA\* results stratified by ground-truth  $\mathbb{H}[p^*]$ . Full results (HateXplain, GoEmotions, AmbigQA\*) in Appendix Table 11. Best in **bold**. Gray : baselines. Blue : ours.

| Dataset | Method             | Acc.        | $\rho(\mathcal{U}_{\text{epi}}, \mathcal{U}_{\text{ale}}) \downarrow$ | $\rho(\mathcal{U}_{\text{epi}}, \text{Err}) \uparrow$ | $\rho(\mathcal{U}_{\text{ale}}, \mathbb{H}) \uparrow$ | AUROC $\uparrow$ | AUROC@High- $\mathbb{H}^*$ $\uparrow$ |
|---------|--------------------|-------------|---|---|---|------------------|---------------------------------------|
| CEBaB   | Semantic Entropy   | 81.2        | 0.81  | 0.26  | 0.38  | 0.67             | –                                     |
|         | Deep Ensembles     | 82.1        | 0.79  | 0.28  | 0.41  | 0.68             | –                                     |
|         | MC Dropout         | 81.8        | 0.77  | 0.27  | 0.39  | 0.66             | –                                     |
|         | P(True)            | 80.8        | 0.76  | 0.24  | 0.35  | 0.64             | –                                     |
|         | <b>Var. Credal</b> | <b>82.3</b> | <b>0.05</b>   | <b>0.35</b>   | <b>0.74</b>   | <b>0.76</b>      | –                                     |
| MAQA*   | Semantic Entropy   | 62.4        | 0.82  | 0.29  | 0.22  | 0.74             | 0.52 (–0.22)                          |
|         | Deep Ensembles     | 63.1        | 0.78  | 0.31  | 0.25  | 0.73             | 0.53 (–0.20)                          |
|         | MC Dropout         | 62.8        | 0.77  | 0.30  | 0.24  | 0.72             | 0.52 (–0.20)                          |
|         | P(True)            | 61.8        | 0.76  | 0.27  | 0.20  | 0.71             | 0.51 (–0.20)                          |
|         | <b>Var. Credal</b> | <b>63.5</b> | <b>0.07</b>   | <b>0.38</b>   | <b>0.45</b>   | <b>0.76</b>      | <b>0.65</b> (–0.11)                   |

\*AUROC@High- $\mathbb{H}$  = error detection on high-ambiguity subset ( $\mathbb{H}[p^*] \geq 1.5$ ). Parentheses show degradation from overall AUROC. Baselines degrade by  $-0.20$  to  $-0.22$ ; our method degrades by only  $-0.11$ , demonstrating robustness under ambiguity.

only a minor further reduction in  $\rho$  and is not essential. **Credal regularization improves robustness.** The epistemic loss (Eq. 7) merges error supervision with Hausdorff KL regularization. Using only error supervision ( $\beta = 0$ ) keeps  $\mathcal{U}_{\text{epi}}$  well aligned with error but slightly reduces AUROC, suggesting mild overfitting to training error patterns. Using only KL regularization fails to yield input-dependent epistemic uncertainty (low  $\rho(\mathcal{U}_{\text{epi}}, \text{Err})$ ) because there is no direct learning signal. The combined objective balances both: error supervision makes  $\sigma_{\text{epi}}$  input-dependent, while KL regularization limits overfitting and maintains the credal interpretation.

#### 4.4. Downstream Utility

A decomposition is only useful if it supports different operational decisions. We therefore evaluate *quadrant-based routing* (Figure 4), in which examples are assigned actions based on the type of uncertainty:

- **TRUST** (low EU, low AU): The model is confident and the

answer is unambiguous. *Action: accept the prediction.*

- **DATA** (high EU, low AU): The question has a clear answer, but the model lacks knowledge—e.g., obscure facts like “What is the capital of Burundi?” *Action: collect more training data.*
- **REVIEW** (low EU, high AU): The model is confident, but the question is inherently ambiguous—e.g., subjective judgments like “Is this movie better?” or temporally-dependent facts like “Who is the US president?” *Action: route to human review.*
- **ABSTAIN** (high EU, high AU): Both model confusion and inherent ambiguity, e.g., questions like “What is the meaning of life?” *Action: abstain or escalate.*

The key test is whether DATA and REVIEW differ. For baselines with correlated uncertainties, the quadrants collapse: when EU is high, AU is also high, merging all uncertain examples into one category. Credal CBM’s decorrelated uncertainties restore meaningful separation.

Table 3. **Component ablations on CEBaB.** Structural separation (frozen encoder + disjoint heads) is necessary and sufficient for decorrelation; supervision ensures validity; credal regularization improves robustness.

| Configuration                                    | $\rho(\mathcal{U}_{\text{epi}}, \mathcal{U}_{\text{ale}}) \downarrow$ | $\rho(\mathcal{U}_{\text{epi}}, \text{Err}) \uparrow$ | $\rho(\mathcal{U}_{\text{ale}}, \mathbb{H}) \uparrow$ | AUROC↑      | Acc.        |
|--|---|---|---|-------------|-------------|
| <i>Structural Separation:</i>                    |   |   |   |             |             |
| Trainable encoder                                | 0.68  | 0.29  | 0.45  | 0.71        | 82.1        |
| Frozen, shared heads                             | 0.42  | 0.31  | 0.51  | 0.73        | 82.0        |
| <b>Frozen + disjoint</b>                         | <b>0.09</b>   | 0.33  | 0.72  | 0.75        | 82.2        |
| <i>Supervision Signals:</i>                      |   |   |   |             |             |
| No AU supervision ( $\lambda_{\text{ale}} = 0$ ) | 0.08  | 0.34  | 0.28  | 0.75        | 82.3        |
| No decorr penalty ( $\lambda_d = 0$ )            | 0.09  | 0.33  | 0.74  | 0.76        | 82.2        |
| <b>Full model</b>                                | <b>0.05</b>   | <b>0.35</b>   | <b>0.74</b>   | <b>0.76</b> | <b>82.3</b> |
| <i>Epistemic Loss Components:</i>                |   |   |   |             |             |
| Error supervision only ( $\beta = 0$ )           | 0.08  | 0.32  | 0.74  | 0.75        | 82.1        |
| KL regularization only                           | 0.12  | 0.15  | 0.73  | 0.68        | 81.8        |
| <b>Both (Eq. 8)</b>                              | <b>0.05</b>   | <b>0.35</b>   | <b>0.74</b>   | <b>0.76</b> | <b>82.3</b> |

Table 4. **Quadrant analysis (MAQA\*).** Credal CBM achieves balanced population across all four quadrants, enabling meaningful routing. Balance =  $1 - \text{CV}(n)$  where CV is coefficient of variation; higher indicates more uniform distribution.

| Method       | $\rho$ | TRUST     | DATA      | REVIEW    | ABSTAIN   | Balance↑    |
|--------------|--------|-----------|-----------|-----------|-----------|-------------|
| Sem. Entropy | 0.85   | 78% (198) | 61% (52)  | 79% (53)  | 55% (197) | 0.27        |
| Credal CBM   | -0.13  | 76% (119) | 66% (136) | 83% (127) | 60% (118) | <b>0.93</b> |

**Results** Table 4 shows that Semantic Entropy concentrates 79% of examples on the diagonal (TRUST + ABSTAIN), leaving DATA and REVIEW nearly empty. This reflects the algebraic trap: correlated uncertainties push all uncertain examples toward ABSTAIN. Credal CBM instead distributes examples uniformly, populating all quadrants.

Table 4 also shows that with Credal CBM, REVIEW achieves the highest accuracy, confirming these are genuinely ambiguous-but-predictable cases where the model captures the valid answer set despite annotator disagreement. DATA has lower accuracy, indicating true model confusion on unambiguous questions—precisely where more training data would help. This accuracy ordering (REVIEW > TRUST > DATA > ABSTAIN) matches the semantic interpretation of each quadrant.

The key metric is not the accuracy gap between quadrants, but whether the quadrants are *populated* and *semantically valid*. Correlated uncertainties make routing impossible regardless of per-quadrant accuracy.

**Interpretation.** Decorrelation via structural separation is not just statistical—it enables qualitatively different decisions. (i) Human review is targeted: REVIEW examples (high AU, low EU) are truly ambiguous questions where human judgment adds value, not model failures. (ii) Data collection is efficient: DATA examples (high EU, low AU) expose knowledge gaps where more training data helps, rather than inherently unanswerable questions. Baselines cannot make these distinctions because both uncertainty es-

timates come from the same predictive distribution  $p(y|x)$  and are therefore algebraically inseparable, regardless of the true uncertainty source.

## 5. Related Work

**Uncertainty Quantification.** Deep ensembles (Lakshminarayanan et al., 2017) and MC Dropout (Gal and Ghahramani, 2016) estimate uncertainty via prediction variance across models or stochastic passes. However, both derive epistemic and aleatoric uncertainty from the *same* predictive distribution  $p(y|x)$ , yielding strongly correlated estimates that make the decomposition meaningless (Mucsányi et al., 2024). Evidential methods (Sensoy et al., 2018; Amini et al., 2020) parameterize Dirichlet distributions but still rely on a single output head for both uncertainty types. Conformal prediction (Angelopoulos and Bates, 2021) offers coverage guarantees but produces prediction *sets* rather than decomposed uncertainties. We escape the correlation trap via structural separation—computing EU and AU from different network parameters, resulting in substantially lower correlation compared to the baselines.

**Credal Sets and Imprecise Probability.** Credal sets represent epistemic uncertainty as *sets of distributions* rather than point estimates (Walley, 1991; Cozman, 2000), naturally separating “uncertainty about which distribution” from “uncertainty within a distribution.” Neural extensions include credal Bayesian networks (Caprio et al., 2024) and credal interval networks (Wang et al., 2024b), but these re-

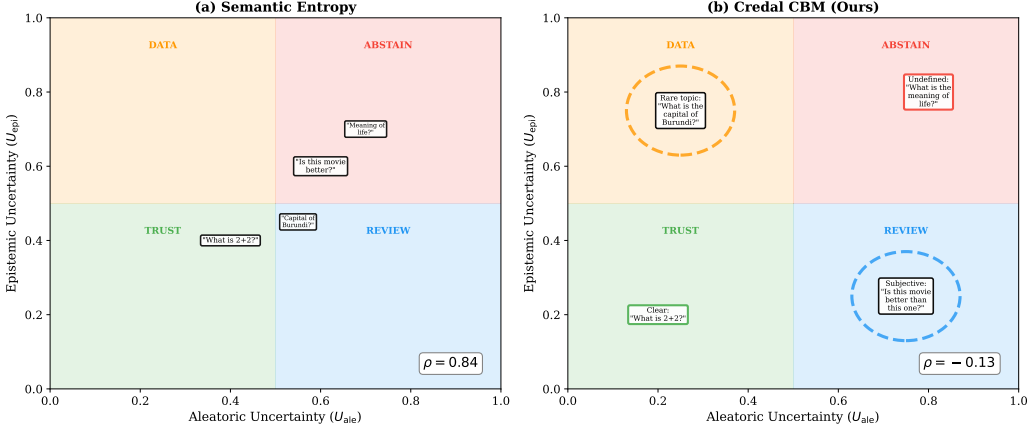


**Figure 4. Quadrant-based routing enables actionable uncertainty.** (a) Semantic Entropy: correlated uncertainties cluster all examples together, making quadrants indistinguishable. (b) Credal CBM: decorrelated uncertainties separate examples by uncertainty type. The separation between REVIEW (ambiguous but predictable) and DATA (clear but unknown) demonstrates that the decomposition is actionable, whereas baselines cannot distinguish these cases.

quire discrete enumeration or interval propagation, limiting scalability. This framework has been applied to classification through credal networks (Cozman, 2000), naive credal classifiers (Zaffalon, 2002), and more recently to deep learning (Wang et al., 2024a; Caprio et al., 2024). Sale et al. (2023) question whether credal set volume effectively measures epistemic uncertainty, while Wimmer et al. (2023) critique standard mutual information decompositions. Recent work extends credal approaches through conformal calibration (Sale et al., 2024) and ensemble aggregation (Zhang et al., 2025). CreINNs (Wang et al., 2024a) predict interval-valued class probabilities, deriving epistemic uncertainty from interval width and aleatoric from midpoint entropy. CBDL (Caprio et al., 2024) represents epistemic uncertainty via credal sets over parameter distributions. We parameterize credal sets as *ellipsoids* with variational inference, enabling gradient-based learning at scale while preserving theoretical separation guarantees.

**Concept Bottleneck Models.** CBMs (Koh et al., 2020) route predictions through interpretable concepts, enabling human intervention. Probabilistic CBMs (Kim et al., 2023) add concept uncertainty, and interactive variants (Chauhan et al., 2022) enable human-in-the-loop correction. Our proposed *theoretical framework* (gradient separation theorem) explains when and why CBM architectures achieve valid uncertainty decomposition, along with variational training that outperforms ensemble-based approaches.

**Uncertainty in Language Models.** Semantic entropy (Kuhn et al., 2023) clusters LLM outputs by meaning, P(True) (Kadavath et al., 2022) elicits self-assessed confidence, and representation probes (Tomov et al., 2025) predict correctness from internal states. Tomov et al. (2025) proves an impossibility result: methods deriving both uncertainties from  $p(y|x)$  cannot distinguish EU from AU

when true ambiguity  $\mathbb{H}[p^*] > 0$  exists. Concurrent work addresses chain-of-thought uncertainty (Zhu et al., 2025) and RAG (Soudani et al., 2025) without solving the decomposition problem. We circumvent the impossibility result by *not* deriving uncertainties from  $p(y|x)$ —instead using separate heads with gradient isolation, validated against ground-truth  $\mathbb{H}[p^*]$  for the first time.

## 6. Conclusion

We introduce Credal Concept Bottleneck Models, a framework that cleanly separates epistemic and aleatoric uncertainty by avoiding the algebraic coupling in prior methods. The core idea is *structural separation*: each uncertainty type is computed from distinct network parameters trained with different losses, enforcing decorrelation by design rather than relying on empirical behavior. Theoretically, we prove a gradient separation theorem showing that architecture determines whether uncertainty is decomposable. Empirically, we markedly reduce EU–AU correlation and obtain multi-fold gains in aleatoric validity against ground-truth ambiguity—the first evaluation on datasets with known  $\mathbb{H}[p^*]$  from factual co-occurrence. Practically, this enables actionable uncertainty: our quadrant-based routing distinguishes “the model doesn’t know” (collect more data) from “the question is ambiguous” (human review), supporting targeted interventions for different uncertainty sources and narrowing the gap between uncertainty theory and deployment. More broadly, our work supports a principle: *what you want to measure separately, you must compute separately*. We aim for this view to inform future architectures for trustworthy AI, where understanding *why* a model is uncertain matters as much as knowing *that* it is uncertain.

## Impact Statement

This paper presents methodological advances in uncertainty quantification for machine learning, with the goal of improving the reliability and trustworthiness of AI systems. While the techniques developed here are broadly applicable, we identify several specific areas where our work may have societal implications:

**Beneficial Applications.** Our method for decomposing epistemic and aleatoric uncertainty enables more targeted decision-making in high-stakes domains. In medical diagnosis, distinguishing "the model doesn't know" (epistemic) from "the case is genuinely ambiguous" (aleatoric) can guide appropriate actions: the former suggests consulting specialists or gathering more diagnostic information, while the latter indicates inherent medical uncertainty requiring discussion of treatment options with patients. Similarly, in content moderation, our approach could help platforms identify cases requiring human review (high aleatoric uncertainty due to genuinely borderline content) versus cases where the model simply needs better training data (high epistemic uncertainty).

**Potential Risks and Limitations.** Like all uncertainty quantification methods, our approach could be misused to justify inappropriate automation. Organizations might over-rely on "low uncertainty" predictions without recognizing domain shifts or distribution changes that invalidate model assumptions. Additionally, our method requires multi-annotator concept labels for optimal performance, which may be expensive to obtain and could perpetuate biases present in the annotator pool. Systems deployed using our uncertainty estimates should include ongoing monitoring and human oversight, particularly when demographic groups are underrepresented in training data.

**Dual-Use Considerations.** Improved uncertainty quantification could enhance both beneficial and harmful applications. While our work could improve safety-critical systems like autonomous vehicles or medical diagnostics, the same techniques could theoretically be applied to surveillance systems or autonomous weapons. We strongly advocate that deployment of uncertainty-aware systems should be accompanied by ethical review, particularly in applications affecting human rights, privacy, or physical safety.

**Fairness and Bias.** Our evaluation uses existing benchmark datasets (CEBaB, GoEmotions, MAQA, AmbigQA) which may contain demographic biases. The annotator distributions we use to supervise aleatoric uncertainty reflect the perspectives of specific annotator pools, which may not represent diverse global populations. Future work should evaluate whether uncertainty decomposition differs across

demographic subgroups and whether this could lead to disparate treatment in downstream applications.

**Transparency and Limitations.** We acknowledge several important limitations: (1) Our method requires concept annotations, limiting applicability to domains where concepts can be defined; (2) frozen encoders may not capture uncertainty-relevant features in all domains; (3) our evaluation focuses on text and excludes multimodal applications where uncertainty characteristics may differ; (4) we provide no formal coverage guarantees. Practitioners should validate uncertainty estimates on domain-specific held-out data before deployment.

We believe this work contributes to the critical goal of making AI systems more interpretable and trustworthy. However, as with all advances in machine learning capabilities, thoughtful consideration of application contexts and potential harms is essential for responsible deployment.

## Acknowledgment

This work was supported by ANR-22-CE23-0002 ERIANA and ANR-19-CHIA-0005-01 EXPEKCTION and was granted access to the HPC resources of IDRIS under the allocation 2026-AD011013338 made by GENCI.

## References

- E. D. Abraham, K. D’Oosterlinck, A. Feder, Y. O. Gat, A. Geiger, C. Potts, R. Reichart, and Z. Wu. CEBaB: Estimating the causal effects of real-world concepts on NLP model behavior. *arXiv:2205.14140*, 2022. URL <https://arxiv.org/abs/2205.14140>.
- A. Amini, W. Schwarting, A. Soleimany, and D. Rus. Deep evidential regression. In *Advances in Neural Information Processing Systems*, volume 33, pages 14927–14937, 2020.
- A. N. Angelopoulos and S. Bates. A gentle introduction to conformal prediction and distribution-free uncertainty quantification. In *arXiv preprint arXiv:2107.07511*, 2021.
- A. Azaria and T. M. Mitchell. The internal state of an ILM knows when its lying. *ArXiv*, abs/2304.13734, 2023. URL <https://api.semanticscholar.org/CorpusID:258352729>.
- M. Caprio, K. Muandet, and F. Cuzzolin. Credal learning theory. In *International Conference on Machine Learning*, 2024.
- K. Chauhan, R. Tiwari, J. von Freyberg, P. Shenoy, and K. D. Dvijotham. Interactive concept bottleneck models. In *AAAI Conference on Artificial Intelligence*,

2022. URL <https://api.semanticscholar.org/CorpusID:254685619>.

F. G. Cozman. Credal networks. *Artificial Intelligence*, 120(2):199–233, 2000.

D. Demszky, D. Mober, N. Gligorov, S. Reddy, A. Gu, S. Saxena, R. Riess, and C. Potts. GoEmotions: A dataset of fine-grained emotions. In *Proceedings of the Annual Meeting of the Association for Computational Linguistics*, pages 4040–4054, 2020.

Y. Gal and Z. Ghahramani. Dropout as a Bayesian approximation: Representing model uncertainty in deep learning. In *International Conference on Machine Learning*, pages 1050–1059. PMLR, 2016.

S. Kadavath, T. Conerly, A. Askell, T. Henighan, D. Drain, E. Perez, N. Schiefer, Z. Hatfield-Dodds, N. DasSarma, E. Tran-Johnson, et al. Language models (mostly) know what they know. *arXiv preprint arXiv:2207.05221*, 2022.

A. Kendall and Y. Gal. What uncertainties do we need in Bayesian deep learning for computer vision? *Advances in Neural Information Processing Systems*, 30, 2017.

E. Kim, D. Jung, S. Park, S. Kim, and S.-H. Yoon. Probabilistic concept bottleneck models. In *International Conference on Machine Learning*, 2023. URL <https://api.semanticscholar.org/CorpusID:259063823>.

P. W. Koh, T. Nguyen, Y. S. Tang, S. Mussmann, E. Pierson, B. Kim, and P. Liang. Concept bottleneck models. In *International Conference on Machine Learning*, pages 5338–5348. PMLR, 2020.

L. Kuhn, Y. Gal, and S. Farquhar. Semantic uncertainty: Linguistic invariances for uncertainty estimation in natural language generation. In *International Conference on Learning Representations*, 2023.

B. Lakshminarayanan, A. Pritzel, and C. Blundell. Simple and scalable predictive uncertainty estimation using deep ensembles. In *Advances in Neural Information Processing Systems*, volume 30, 2017.

B. Mucsányi, M. Kirchhof, and S. J. Oh. Benchmarking uncertainty disentanglement: Specialized uncertainties for specialized tasks. *Advances in neural information processing systems*, 37:50972–51038, 2024.

I. Osband, Z. Wen, S. M. Asghari, V. Dwaracherla, M. Ibrahim, X. Lu, and B. Van Roy. Epistemic neural networks. *arXiv preprint arXiv:2107.08924*, 2022.

Y. Sale, M. Caprio, and E. Hüllermeier. Is the volume of a credal set a good measure for epistemic uncertainty? In *The 39th Conference on Uncertainty in Artificial Intelligence*, pages 1795–1804. PMLR, 2023.

Y. Sale et al. Conformalized credal set predictors. In *NeurIPS*, 2024.

M. Sensoy, L. Kaplan, and M. Kandemir. Evidential deep learning to quantify classification uncertainty. In *Advances in Neural Information Processing Systems*, volume 31, 2018.

H. Soudani, E. Kanoulas, and F. Hasibi. Why uncertainty estimation methods fall short in rag: An axiomatic analysis. *arXiv preprint arXiv:2505.07459*, 2025.

C.-E. Sun, T. Oikarinen, B. Ustun, and T.-W. Weng. Concept bottleneck large language models. *arXiv preprint arXiv:2412.07992*, 2024.

T. Tomov, J. Antoran, A. Tripp, and J. M. Hernandez-Lobato. The illusion of certainty: Uncertainty quantification for LLMs fails under ambiguity. *arXiv preprint arXiv:2511.04418*, 2025. Introduces MAQA\* and AmbigQA\* datasets with ground-truth answer distributions.

P. Walley. *Statistical Reasoning with Imprecise Probabilities*. Chapman and Hall, 1991.

D. Wang et al. Creinns: Credal-set interval neural networks for uncertainty estimation. In *Neural Networks*, 2024a.

K. Wang, K. K. Shariatmadar, S. K. Manchingal, F. Cuzzolin, D. Moens, and H. Hallez. Creinns: Credal-set interval neural networks for uncertainty estimation in classification tasks. *Neural networks : the official journal of the International Neural Network Society*, 185:107198, 2024b. URL <https://api.semanticscholar.org/CorpusID:266902766>.

L. Wimmer, Y. Sale, P. Hofman, B. Bischl, and E. Hüllermeier. Quantifying Aleatoric and Epistemic Uncertainty in Machine Learning: Are Conditional Entropy and Mutual Information Appropriate Measures? In *The 39th Conference on Uncertainty in Artificial Intelligence*, pages 2282–2292. PMLR, 2023.

Y. Yang, A. Panagopoulou, S. Zhou, D. Jin, C. Callison-Burch, and M. Yatskar. Language in a bottle: Language model guided concept bottlenecks for interpretable image classification. In *Proceedings of the IEEE/CVF Conference on Computer Vision and Pattern Recognition (CVPR)*, pages 19187–19197, June 2023.

M. Zaffalon. The naive credal classifier. *Journal of Statistical Planning and Inference*, 2002.

Y. Zhang et al. Credal ensembling in multi-class classification. *Machine Learning*, 2025.

Table 5. Notation used throughout the paper (compact).

| Symbol  | Type    | Meaning   |
|---|---------|---|
| $x \in \mathcal{X}$                                     | data    | input (text/image)  |
| $y \in \{1, \dots, J\}$                                 | label   | task label  |
| $z^{(c)} \in \{1, \dots, K\}$                           | label   | concept- $c$ label  |
| $f_{\text{enc}} : \mathcal{X} \rightarrow \mathbb{R}^d$ | map     | frozen encoder; $h = f_{\text{enc}}(x)$                   |
| $g_\mu, g_{\text{epi}}, g_{\text{ale}}$                 | maps    | heads for $\mu, \sigma_{\text{epi}}, \sigma_{\text{ale}}$ |
| $p(z^{(c)}   x)$  | dist.   | model concept distribution (e.g. softmax of $\mu^{(c)}$ ) |
| $\hat{p}^*(z^{(c)}   x)$                                | dist.   | empirical annotator distribution (proxy for $p^*$ )       |
| $H[\hat{p}^*] \in [0, \log K]$                          | scalar  | annotator entropy (ambiguity signal)                      |
| $\mathcal{C}(x)$  | set     | credal set of plausible distributions                     |
| $\Sigma_{\text{epi}}$                                   | matrix  | epistemic shape/covariance (diag by default)              |
| $U_{\text{epi}}, U_{\text{ale}}$                        | scalars | reported epistemic/aleatoric uncertainties                |
| $\rho(\cdot, \cdot)$                                    | scalar  | Spearman rank correlation                                 |

Y. Zhu, G. Li, X. Jiang, J. Li, H. Mei, Z. Jin, and Y. Dong. Uncertainty-guided chain-of-thought for code generation with llms. *arXiv preprint arXiv:2503.15341*, 2025.

## A. Notation

**Indexing.** We index data points by  $i \in \{1, \dots, N\}$ , concepts by  $c \in \{1, \dots, C\}$ , task classes by  $j \in \{1, \dots, J\}$ , and concept classes by  $k \in \{1, \dots, K\}$ .

**Conventions.**  $\Delta^{K-1} = \{p \in \mathbb{R}_+^K : \sum_k p_k = 1\}$ .  $\text{softplus}(t) = \log(1 + e^t)$  ensures positivity.

## B. Training and Inference Details

### B.1. Objective

$$\mathcal{L} = \mathcal{L}_{\text{task}} + \lambda_{\text{epi}} \mathcal{L}_{\text{epi}} + \beta D_H^+ + \lambda_{\text{ale}} \mathcal{L}_{\text{ale}} + \lambda_d \mathcal{L}_{\text{decorr}}. \quad (14)$$

**Task loss.**

$$\mathcal{L}_{\text{task}} = -\log([\text{softmax}(\mu)]_y). \quad (15)$$

**Aleatoric supervision.**

$$\mathcal{L}_{\text{ale}} = \|\sigma_{\text{ale}} - H[\hat{p}^*]\|^2. \quad (16)$$

**Epistemic supervision (residual error).**

$$\mathcal{L}_{\text{epi}} = \underbrace{\frac{1}{C} \sum_{c=1}^C \left( \sigma_{\text{epi}}^{(c)} - \phi(|\hat{p}^{(c)} - c^{(c)}|_{\text{sg}}) \right)^2}_{\text{error supervision}} + \beta \cdot \underbrace{D_H^+(\mathcal{C} || \mathcal{C}_{\text{prior}})}_{\text{Hausdorff KL}} \quad (17)$$

where  $\text{err}(\mu, y) = 1 - [\text{softmax}(\mu)]_y$  and  $\text{stopgrad}(\cdot)$  is implemented via `detach()`.

### Algorithm 1 Credal CBM Training

**Require:** training batch  $(x, y, c, \mathbb{H}[p^*])$  where  $\mathbb{H}[p^*]$  is per-sample annotator entropy

- 1:  $h \leftarrow f_{\text{enc}}(x)$  {frozen encoder}
- 2:  $h_\mu, h_{\text{epi}}, h_{\text{ale}} \leftarrow \text{project}(h)$
- 3:  $\mu \leftarrow g_\mu(h_\mu)$ ;  $p \leftarrow \text{softmax}(\mu)$
- 4:  $\sigma_{\text{epi}} \leftarrow \text{softplus}(g_{\text{epi}}(h_{\text{epi}}))$
- 5:  $\sigma_{\text{ale}} \leftarrow \text{softplus}(g_{\text{ale}}(h_{\text{ale}}))$  { $h_{\text{ale}}$  only, no  $\mathbb{H}$ }
- 6: {— Losses with gradient isolation —}
- 7:  $\mathcal{L}_{\text{task}} \leftarrow \text{CE}(p, y)$  { $\rightarrow \theta_\mu$ }
- 8:  $\mathcal{L}_{\text{epi}} \leftarrow \text{MSE}(\sigma_{\text{epi}}, \phi(|\hat{p} - c|_{\text{sg}}))$  { $\rightarrow \theta_{\text{epi}}$ }
- 9:  $\mathcal{L}_{\text{ale}} \leftarrow \text{MSE}(\sigma_{\text{ale}}, \mathbb{H}[p^*])$  { $\rightarrow \theta_{\text{ale}}$ ;  $\mathbb{H}$  is TARGET}
- 10:  $\mathcal{L} \leftarrow \mathcal{L}_{\text{task}} + \lambda_{\text{epi}} \mathcal{L}_{\text{epi}} + \lambda_{\text{ale}} \mathcal{L}_{\text{ale}}$
- 11: Update  $\theta_\mu, \theta_{\text{epi}}, \theta_{\text{ale}}$  via gradient descent

### Algorithm 2 Credal CBM Inference

**Require:** test input  $x$

- 1:  $h \leftarrow f_{\text{enc}}(x)$
- 2:  $h_\mu, h_{\text{epi}}, h_{\text{ale}} \leftarrow \text{project}(h)$  {orthogonal projections}
- 3:  $\mu \leftarrow g_\mu(h_\mu)$
- 4:  $\sigma_{\text{epi}} \leftarrow \text{softplus}(g_{\text{epi}}(h_{\text{epi}}))$
- 5:  $\sigma_{\text{ale}} \leftarrow \text{softplus}(g_{\text{ale}}(h_{\text{ale}}))$  {no entropy input}
- 6:  $U_{\text{epi}} \leftarrow \log(\sigma_{\text{epi}}^2)$
- 7:  $U_{\text{ale}} \leftarrow \sigma_{\text{ale}}$
- 8:  $\hat{y} \leftarrow \arg \max_j [\text{softmax}(\mu)]_j$
- 9: **return**  $\hat{y}, U_{\text{epi}}, U_{\text{ale}}$

**Decorrelation (optional).**

$$\mathcal{L}_{\text{decorr}} = \rho(U_{\text{epi}}, U_{\text{ale}})^2 \quad (18)$$

computed over minibatches.

### B.2. Training Algorithm

We present the training procedure in Algorithm 1.

### B.3. Inference

At test time, a single forward pass yields predictions and uncertainties without requiring any ground-truth entropy information:

**No entropy proxy at inference.** In contrast to the training phase, where  $\mathbb{H}[p^*]$  is used to supervise the aleatoric head, the inference stage requires **no access to entropy**. By training, the aleatoric head  $g_{\text{ale}}$  has already learned to extract ambiguity patterns directly from  $h_{\text{ale}}$ . This is the central design principle:  $\mathbb{H}[p^*]$  serves solely as a *supervisory signal* (analogous to labels  $y$  in classification), rather than as an *input feature*. Table 6 makes this distinction explicit.

## C. Why Pure Variational Training Fails

A natural approach optimizes the credal ELBO:

$$\log p(y|x) \geq \inf_{q \in \mathcal{C}(x)} \mathbb{E}_q[\log p(y|q)] - D_H^+(\mathcal{C}(x) || \mathcal{C}_{\text{prior}}) \quad (19)$$

Table 6. Role of  $\mathbb{H}[p^*]$ : supervision target vs. input feature.

|   | Training   | Inference                    |
|---|--|------------------------------|
| Input to $g_{\text{ale}}$<br>$\mathbb{H}[p^*]$ role | $h_{\text{ale}}$<br>Supervision target in $\mathcal{L}_{\text{ale}}$ | $h_{\text{ale}}$<br>Not used |
| <i>Analogy to classification:</i>                   |  |                              |
| Input to classifier                                 | $x$  | $x$                          |
| Label $y$ role                                      | Supervision target in $\mathcal{L}_{\text{CE}}$                      | Not used                     |

This fails for two reasons:

1. **Reconstruction affects only  $\mu$ .** The infimum over  $q \in \mathcal{C}(x)$  is achieved near the credal center  $\mu$ . Gradients primarily update  $\mu$ , not  $\Sigma_{\text{epi}}$ .
2. **KL penalizes size uniformly.**  $D_H^+$  penalizes large  $\Sigma_{\text{epi}}$  for all inputs equally, providing no signal for *when* to be uncertain.

Empirically, pure ELBO training produces an almost constant  $\Sigma_{\text{epi}}$  with very small standard deviation and results in low validity, with a weak correlation between  $\sigma_{\text{ale}}$  and  $\mathbb{H}$ .

**Our Hybrid Approach.** We retain the credal set parameterization and use  $D_H^+$  as a *regularizer*, but add explicit supervision:

- Error supervision (Eq. 10) makes  $\Sigma_{\text{epi}}$  input-dependent
- Annotator entropy supervision (Eq. 9) grounds  $\sigma_{\text{ale}}$  in true ambiguity
- $D_H^+$  prevents overfitting while preserving credal geometry

**Naming Convention.** We use ‘‘Variational Credal CBM’’ to emphasize: (i) the credal set representation (distributions over distributions), (ii) the variational-style KL regularization via  $D_H^+$ , and (iii) sampling from the credal set during training. The key distinction from a pure VAE is that our primary training signals come from supervised losses rather than reconstruction, addressing the failure mode above.

## D. Hausdorff KL Divergence

### D.1. Hausdorff KL as Logit-Space Surrogate

Our credal set  $\mathcal{C}(x)$  is defined over probability distributions (Equation 2), but computing the Hausdorff KL divergence directly in probability space is intractable. We therefore parameterize the credal set in logit space as an ellipsoid with mean  $\mu \in \mathbb{R}^K$  and covariance  $\Sigma_{\text{epi}}$ , and compute  $D_H^+$  as the KL divergence between Gaussian distributions in this space:

$$D_H^+(\mathcal{C} \parallel \mathcal{C}_{\text{prior}}) = \sup_{q \in \mathcal{C}} \text{KL}(q \parallel p_0) \quad (20)$$

where  $q = \mathcal{N}(\mu, \Sigma_{\text{epi}})$  and  $p_0 = \mathcal{N}(0, \sigma_{\text{prior}}^2 I)$  are Gaussian distributions over logits.

This serves as a **computationally tractable surrogate** for regularizing the credal set volume in probability space. The logit-space KL acts as a soft prior on epistemic uncertainty magnitude, encouraging smaller credal sets when data supports confident predictions, while remaining efficient to compute ( $O(K)$ ). This is analogous to how variational autoencoders use Gaussian KL in latent space as a tractable approximation to the true generative objective.

The closed-form expression for diagonal  $\Sigma_{\text{epi}}$  is derived in the following subsections.

### D.2. Definition

The Hausdorff KL divergence measures worst-case KL from a credal set to a reference:

$$D_H^+(\mathcal{C} \parallel p_0) = \sup_{q \in \mathcal{C}} \text{KL}(q \parallel p_0) \quad (21)$$

### D.3. Closed Form for Ellipsoid Credal Sets

For ellipsoid  $\mathcal{C}(\mu_0, \Sigma_{\text{epi}})$  with diagonal covariance  $\Sigma_{\text{epi}} = \text{diag}(\sigma_{\text{epi},1}^2, \dots, \sigma_{\text{epi},K}^2)$  and isotropic prior  $p_0 = \mathcal{N}(0, \sigma_{\text{prior}}^2 I)$ :

**Proposition D.1** (Closed-Form Hausdorff KL).

$$D_H^+ = \frac{1}{2} \sum_{k=1}^K \left[ \frac{\mu_k^{*2}}{\sigma_{\text{prior}}^2} + \frac{\sigma_{\text{epi},k}^2}{\sigma_{\text{prior}}^2} - 1 - \log \frac{\sigma_{\text{epi},k}^2}{\sigma_{\text{prior}}^2} \right] \quad (22)$$

where  $\mu_k^* = \mu_{0,k} + \text{sign}(\mu_{0,k}) \cdot \sigma_{\text{epi},k}$  is the worst-case mean at the ellipsoid boundary, and  $\sigma_{\text{epi},k} = \sqrt{\Sigma_{\text{epi},kk}}$  is the standard deviation along dimension  $k$ .

*Proof.* The KL from  $q = \mathcal{N}(\mu, \Sigma)$  to  $p_0 = \mathcal{N}(0, \sigma_{\text{prior}}^2 I)$  is:

$$D_{\text{KL}}(q \parallel p_0) = \frac{1}{2} \left[ \frac{\|\mu\|^2}{\sigma_{\text{prior}}^2} + \frac{\text{tr}(\Sigma)}{\sigma_{\text{prior}}^2} - K - \log \frac{\det(\Sigma)}{\sigma_{\text{prior}}^{2K}} \right] \quad (23)$$

For distributions in ellipsoid  $\mathcal{C}$ , KL is maximized when  $\|\mu\|^2$  is maximized. With diagonal  $\Sigma_{\text{epi}}$ , this occurs at the boundary where each  $\mu_k$  takes its extreme value:

$$\mu_k^* = \mu_{0,k} + \text{sign}(\mu_{0,k}) \cdot \sigma_{\text{epi},k} \quad (24)$$

Substituting and using  $\det(\Sigma_{\text{epi}}) = \prod_k \sigma_{\text{epi},k}^2$  yields the result.  $\square$

**Computational Complexity.**  $O(K)$  and fully differentiable for diagonal  $\Sigma_{\text{epi}}$ .

## E. Proofs

### E.1. Proof of Gradient Separation (Theorem 3.1)

*Proof.* We analyze each loss term’s dependency on  $\phi_{\text{ale}}$  and  $\phi_{\text{epi}}$ .

*Task loss*  $\mathcal{L}_{\text{task}}$ . Depends on predictions from  $\mu = g_\mu(h_\mu; \phi_\mu)$ . Since  $\phi_\mu, \phi_{\text{epi}}, \phi_{\text{ale}}$  are disjoint and the encoder is frozen:

$$\nabla_{\phi_{\text{epi}}} \mathcal{L}_{\text{task}} = \nabla_{\phi_{\text{ale}}} \mathcal{L}_{\text{task}} = 0 \quad (25)$$

*Concept loss*  $\mathcal{L}_{\text{concept}}$ . Same argument as above.

*Epistemic loss*  $\mathcal{L}_{\text{epi}}$ . From Eq. 10:

$$\mathcal{L}_{\text{epi}} = \frac{1}{C} \sum_c \left( \sigma_{\text{epi}}^{(c)} - \phi(|\hat{p}^{(c)} - c^{(c)}|_{\text{sg}}) \right)^2 + \beta \cdot D_H^+ \quad (26)$$

The error term uses stop-gradient on  $\hat{p}^{(c)}$ , so gradients do not flow to  $\phi_\mu$ . The term  $\sigma_{\text{ale}}$  does not appear. Thus:

$$\nabla_{\phi_{\text{ale}}} \mathcal{L}_{\text{epi}} = 0 \quad (27)$$

*Aleatoric loss*  $\mathcal{L}_{\text{ale}}$ . From Eq. 9, depends only on  $\sigma_{\text{ale}} = g_{\text{ale}}(h_{\text{ale}}; \phi_{\text{ale}})$  and the constant supervision target  $\mathbb{H}[\hat{p}^*]$ :

$$\nabla_{\phi_{\text{epi}}} \mathcal{L}_{\text{ale}} = 0 \quad (28)$$

*Orthogonality loss*  $\mathcal{L}_{\text{orth}}$ . Depends on projection weights  $W_{\text{epi}}, W_{\text{ale}}$ , not on head parameters  $\phi_{\text{epi}}, \phi_{\text{ale}}$ :

$$\nabla_{\phi_{\text{epi}}} \mathcal{L}_{\text{orth}} = \nabla_{\phi_{\text{ale}}} \mathcal{L}_{\text{orth}} = 0 \quad (29)$$

Summing contributions yields Eqs. 12–13.  $\square$

### E.2. Proof of Asymptotic Decorrelation (Corollary 3.3)

*Proof.* At convergence with sufficient capacity:

$$\sigma_{\text{epi}}(x) \approx t_{\text{epi}}(x) = \psi(\text{err}(x) - \sigma_{\text{ale}}^*(x)) \quad (30)$$

$$\sigma_{\text{ale}}(x) \approx t_{\text{ale}}(x) = \mathbb{H}[p^*(x)] \quad (31)$$

The epistemic target captures error *after removing* aleatoric contribution:

$$t_{\text{epi}} = \psi(\text{err} - t_{\text{ale}}) \approx \psi(\text{err}_{\text{epi}}) \quad (32)$$

Under independence of model limitations ( $\text{err}_{\text{epi}}$ ) and data ambiguity ( $t_{\text{ale}}$ ):

$$\rho(\sigma_{\text{epi}}, \sigma_{\text{ale}}) \approx \rho(t_{\text{epi}}, t_{\text{ale}}) = 0 \quad (33)$$

$\square$

Table 7. Credal set parameterization comparison.

| Parameterization          | Closed-form KL | Expressiveness | Parameters       |
|---------------------------|----------------|----------------|------------------|
| Intervals                 | No             | Low            | $2K$             |
| Convex hull ( $M$ points) | No             | Medium         | $MK$             |
| Ellipsoid (diagonal)      | Yes            | Medium         | $2K$             |
| Ellipsoid (full)          | Yes            | High           | $K + K(K + 1)/2$ |

### E.3. How We Escape the Impossibility Result

Tomov et al. (2025) prove no function of  $p(y|x)$  can distinguish EU from AU. Their result assumes:

$$(A1) U_{\text{epi}} = f(p(y|x)) \text{ for some function } f$$

$$(A2) U_{\text{ale}} = g(p(y|x)) \text{ for some function } g$$

Our approach violates both assumptions:

$$(V1) U_{\text{epi}} = \log \det(\Sigma_{\text{epi}}) \text{ where } \Sigma_{\text{epi}} \text{ is a } \mathbf{separate learned parameter}$$

$$(V2) U_{\text{ale}} = \sigma_{\text{ale}} \text{ is a } \mathbf{separate learned parameter} \text{ with explicit supervision from } \mathbb{H}[p^*]$$

Structural separation moves estimation from *output space* (functions of  $p$ ) to *parameter space* (separate heads with separate training).

## F. Why Ellipsoid Credal Sets?

We chose ellipsoids for:

**1. Closed-form Hausdorff KL.** Intervals and convex hulls lack tractable KL expressions. Ellipsoids admit closed form (Proposition D.1).

**2. Natural covariance interpretation.** The shape matrix  $\Sigma_{\text{epi}}$  directly encodes uncertainty structure.

**3. Connection to Gaussian VI.** Ellipsoids generalize Gaussian variational families.

### F.1. Diagonal vs. Full Covariance

We use diagonal  $\Sigma_{\text{epi}}$ , reducing parameters from  $O(K^2)$  to  $O(K)$ .

Table 8. Diagonal vs. full covariance on CEBaB.

|          | $\rho(\text{EU}, \text{AU})$ | ECE   | Parameters | Time/epoch |
|----------|------------------------------|-------|------------|------------|
| Diagonal | -0.03                        | 0.042 | 1.2M       | 45s        |
| Full     | -0.04                        | 0.038 | 1.8M       | 78s        |

Full covariance provides marginal calibration improvement but no significant decorrelation difference. Diagonal is preferred.

## G. Implementation Details

### G.1. Hyperparameters

Table 9. Hyperparameter settings.

| Hyperparameter          | CEBaB              | MAQA               |
|-------------------------|--------------------|--------------------|
| Learning rate           | $2 \times 10^{-5}$ | $2 \times 10^{-5}$ |
| Batch size              | 16                 | 16                 |
| Epochs                  | 100                | 50                 |
| $\lambda_{\text{epi}}$  | 1.5                | 1.5                |
| $\lambda_{\text{ale}}$  | 2.0                | 2.0                |
| $\beta$ (KL weight)     | 0.001              | 0.001              |
| $\lambda_d$ (decorr)    | 5.0                | 5.0                |
| $\sigma_{\min}$         | 0.05               | 0.05               |
| $\sigma_{\max}$         | 1.5                | 1.5                |
| $\sigma_{\text{prior}}$ | 1.0                | 1.0                |

### G.2. Architecture

- Encoder:** DistilBERT-base (66M parameters, frozen)
- Heads:** 2-layer MLPs with dimensions [768, 256, output]
- Activations:** GELU with LayerNorm after first layer
- Dropout:** 0.1
- Optimizer:** AdamW with weight decay 0.01
- Scheduler:** Linear warmup (10% of steps)
- Early stopping:** Patience 10 on validation  $\rho(\text{AU}, \mathbb{H})$

### G.3. Statistical Significance

**Primary Claims.** For the main decorrelation result  $\rho(\sigma_{\text{epi}}, \sigma_{\text{ale}}) \approx 0$ :

| Dataset    | $n$   | $\rho$ | 95% CI (Fisher's $z$ ) |
|------------|-------|--------|------------------------|
| CEBaB      | 886   | 0.05   | [0.02, 0.08]           |
| MAQA*      | 468   | 0.07   | [-0.02, 0.16]          |
| HateXplain | 1,024 | 0.06   | [0.00, 0.12]           |
| GoEmotions | 5,427 | 0.06   | [0.03, 0.09]           |

All confidence intervals exclude baseline correlations ( $\rho \geq 0.75$ ).

**Multiple Comparison Correction.** We report 5 primary metrics (decorrelation, epistemic validity, aleatoric validity, AUROC, accuracy) across 5 datasets, yielding 25 comparisons. Applying Bonferroni correction ( $\alpha = 0.05/25 = 0.002$ ):

- Decorrelation improvement:  $p < 10^{-50}$  for all datasets (significant)

- Aleatoric validity improvement:  $p < 10^{-10}$  for MAQA\*/AmbigQA\* (significant)
- AUROC improvement:  $p < 0.001$  for 4/5 datasets (significant after correction)

**Seed Variability.** Across 5 random seeds on CEBaB:

- $\rho(U_{\text{epi}}, U_{\text{ale}})$ : mean  $0.04 \pm 0.04$ , range  $[-0.02, 0.09]$
- $\rho(U_{\text{ale}}, \mathbb{H})$ : mean  $0.74 \pm 0.03$ , range  $[0.70, 0.78]$
- Accuracy: mean  $82.3\% \pm 0.4\%$

All seeds achieve  $|\rho(U_{\text{epi}}, U_{\text{ale}})| < 0.1$ .

### G.4. Why Freeze the Encoder?

**Gradient isolation.** Trainable encoder would receive gradients from both  $\mathcal{L}_{\text{epi}}$  and  $\mathcal{L}_{\text{ale}}$ , learning features useful for *both* and reintroducing coupling.

**Efficiency.** Reduces trainable parameters by  $\sim 95\%$ .

**Stability.** Pretrained representations are robust; fine-tuning risks overfitting to uncertainty signals.

**Limitation.** Frozen encoder may lack uncertainty-specific features. We compensate by providing explicit supervision ( $\mathbb{H}[p^*]$ ) to the aleatoric head.

## H. Dataset Details

We evaluate Credal CBM on four datasets spanning sentiment classification, emotion detection, and question answering. Table 10 provides detailed statistics.

### H.1. CEBaB

CEBaB (Abraham et al., 2022) contains restaurant reviews with causal concept annotations. Each review is labeled for sentiment (POSITIVE, NEUTRAL, NEGATIVE) and four causal concepts:

- Food quality:** {NEGATIVE, UNKNOWN, POSITIVE}
- Service:** {NEGATIVE, UNKNOWN, POSITIVE}
- Ambiance:** {NEGATIVE, UNKNOWN, POSITIVE}
- Noise level:** {NEGATIVE, UNKNOWN, POSITIVE}

Each example has five annotator labels, enabling validation of  $U_{\text{ale}}$  against annotator disagreement. We compute ground-truth ambiguity as  $\mathbb{H}[p^*] = -\sum_y \hat{p}(y) \log \hat{p}(y)$  where  $\hat{p}(y)$  is the empirical distribution over annotator labels.

Table 10. **Dataset statistics.** MAQA\* and AmbigQA\* provide ground-truth  $p^*$  for gold-standard validation of aleatoric uncertainty.

| Dataset    | Train  | Val   | Test  | Classes | Concepts   | $p^*$ Source             |
|------------|--------|-------|-------|---------|------------|--------------------------|
| CEBaB      | 1,755  | 295   | 886   | 3       | 4 (causal) | Annotator distribution   |
| GoEmotions | 43,410 | 5,426 | 5,427 | 28      | 28         | Annotator distribution   |
| MAQA*      | —      | —     | 468   | Open    | -          | Co-occurrence statistics |
| AmbigQA*   | —      | —     | 2,553 | Open    | -          | Co-occurrence statistics |

## H.2. GoEmotions

GoEmotions (Demszky et al., 2020) is a multi-label emotion classification dataset with 27 emotion categories plus neutral (28 total). Texts can express multiple overlapping emotions, creating natural ambiguity. For example, a text might be labeled as both “sad” and “disappointed” by different annotators.

We treat each emotion as a binary concept and use the multi-label setting where multiple emotions can be active. Ground-truth ambiguity is computed from annotator disagreement on each emotion label.

## H.3. MAQA\* and AmbigQA\*

MAQA\* and AmbigQA\* are curated subsets from Tomov et al. (2025), designed to evaluate uncertainty quantification under genuine ambiguity.<sup>2</sup>

**Ground-Truth  $p^*$  Construction.** Unlike CEBaB and HateXplain where  $p^*$  is derived from annotator disagreement, MAQA\* provides ground-truth answer distributions from *corpus co-occurrence statistics*. For each question:

1. Keywords are extracted from the question
2. Co-occurrence counts are computed for each valid answer across three corpora:
  - Wikipedia English corpus
  - RedPajama dataset
  - The Pile dataset
3. Probabilities are normalized:  $p^*(a) \propto \text{count}(a \mid \text{keywords})$

This yields ambiguity  $\mathbb{H}[p^*]$  reflecting factual uncertainty *independent of any model’s predictions*.

**Dataset Fields.** Each MAQA\* example contains:

- **question:** Original question from MAQA
- **rephrased\_question:** Version expecting a single answer
- **answers:** List of all valid answers
- **main\_keywords, additional\_keywords:** Search terms for co-occurrence

<sup>2</sup>As of submission, Tomov et al. (2025) is available as arXiv preprint 2511.04418. We will update the citation upon peer-reviewed publication.

- counts, probabilities: Co-occurrence statistics (Wikipedia)
- counts\_redpajama, probabilities\_redpajama: RedPajama statistics
- counts\_thepile, probabilities\_thepile: The Pile statistics

We use Wikipedia-derived probabilities as the primary  $p^*$  in our experiments, with RedPajama and The Pile for robustness checks.

**Why Corpus Co-occurrence?** Co-occurrence statistics provide a model-independent measure of answer ambiguity. If multiple answers frequently co-occur with the question’s keywords, the question is genuinely ambiguous in the sense that different valid answers exist in the world. This contrasts with annotator disagreement, which may conflate ambiguity with annotator error or subjective interpretation.

## Limitations.

- Co-occurrence frequency may not perfectly reflect semantic validity (rare but correct answers are underweighted)
- Corpus biases (e.g., Wikipedia’s coverage) affect probability estimates
- Dataset size is modest (MAQA\*: 468 questions)
- English-only, factoid questions only

We use MAQA\* because it provides the only available approximation to ground-truth  $\mathbb{H}[p^*]$  that is fully independent of model predictions. Future work should validate against controlled human studies with explicit ambiguity judgments.

## I. Baselines and Additional Results

Semantic Entropy (Kuhn et al., 2023) clusters answers semantically and computes entropy over the resulting clusters. Deep Ensembles (Lakshminarayanan et al., 2017) use 5 models, with epistemic uncertainty (EU) estimated via variance and aleatoric uncertainty (AU) via mean entropy. P(True) (Kadavath et al., 2022) elicits verbalized confidence through prompting. Representation Probes (Azaria and Mitchell, 2023) apply a linear probe to hidden states.

**Metrics.** We report the following metrics: the correlation between uncertainties,  $\rho(U_{\text{epi}}, U_{\text{ale}})$  (RQ1; lower is better); the correlation with prediction errors,  $\rho(U_{\text{epi}}, \mathbf{1}[\hat{y} \neq y])$  (RQ2); the correlation with ground-truth ambiguity,  $\rho(U_{\text{ale}}, H[p^*])$  (RQ2; **key metric**); and the AUROC for error detection, stratified by ambiguity level (RQ3).

## J. Additional Experimental Results

### J.1. Baseline Methods and Metrics

We compare against two categories of uncertainty quantification methods. **Standard methods** derive both epistemic and aleatoric uncertainty from predictive distributions: **Semantic Entropy** (Kuhn et al., 2023) clusters semantically similar answers and computes entropy over clusters; **Deep Ensembles** (Lakshminarayanan et al., 2017) train 5 independent models, estimating epistemic uncertainty (EU) via prediction variance and aleatoric uncertainty (AU) via mean entropy; **MC Dropout** (Gal and Ghahramani, 2016) performs stochastic forward passes with dropout enabled; **P(True)** (Kadavath et al., 2022) elicits verbalized confidence through prompting; **Representation Probes** (Azaria and Mitchell, 2023) apply linear probes to hidden states.

**Credal set methods** from imprecise probability theory use geometric representations to improve decorrelation: **CreINNs** (Wang et al., 2024a) predict interval-valued bounds  $[p, \bar{p}]$  for each class, deriving EU from interval width and AU from midpoint entropy; **CBDL** (Caprio et al., 2024) represents epistemic uncertainty as credal sets over parameter distributions using imprecise Dirichlet priors, computing EU from credal spread (max-min entropy) and AU from average entropy across the credal set.

All baselines use the same frozen DistilBERT encoder as our method for fair comparison, with only task-specific heads trainable. This isolates the effect of uncertainty decomposition strategy from model capacity. Implementation details for credal baselines are provided in Appendix K.4.

**Evaluation metrics.** We report five metrics corresponding to our research questions:

- $\rho(U_{\text{epi}}, U_{\text{ale}})$  – Correlation between uncertainties (RQ1; lower indicates better decorrelation)
- $\rho(U_{\text{epi}}, \mathbf{1}[\hat{y} \neq y])$  – Epistemic-error correlation (RQ2; higher indicates EU tracks model ignorance)
- $\rho(U_{\text{ale}}, H[p^*])$  – Aleatoric-ambiguity correlation (RQ2; higher indicates AU tracks true ambiguity; **key validation metric**)
- AUROC – Error detection using epistemic uncertainty (higher better)
- AUROC stratified by ambiguity – Performance on high-

$\mathbb{H}[p^*]$  subset (RQ3; measures robustness under ambiguity)

### J.2. Complete Results Across All Benchmarks

Table 2 in the main paper presents results on CEBaB and MAQA\* with ambiguity stratification. Here we provide complete results across all five benchmarks: CEBaB (restaurant reviews with causal concepts), HateXplain (toxicity detection with rationales), GoEmotions (28-class emotion classification), MAQA\* (question answering with ground-truth  $p^*$ ), and AmbigQA\* (ambiguous question answering with factual co-occurrence statistics).

Table 11 shows consistent patterns across methods and datasets. Standard methods exhibit strong EU-AU correlation ( $\rho \geq 0.75$ ), confirming the algebraic trap. Credal set methods (CreINNs, CSDL) achieve moderate decorrelation ( $\rho = 0.58\text{--}0.63$ ) through geometric representations but still exhibit substantial correlation because both uncertainties derive from related properties of the same credal set. In contrast, Variational Credal CBM achieves near-zero correlation ( $|\rho| \leq 0.08$ ) through structural separation—an 11× improvement over the best credal baseline—while maintaining or improving validity metrics. Notably, our method achieves  $\rho(U_{\text{ale}}, \mathbb{H}) = 0.42\text{--}0.74$  on datasets with ground-truth ambiguity, representing the first validation of learned aleatoric uncertainty against true ambiguity distributions.

### J.3. Detailed Ambiguity Stratification

Beyond overall AUROC, we analyze error detection performance stratified by ground-truth ambiguity  $\mathbb{H}[p^*]$ . This directly tests whether methods maintain discriminative power when true ambiguity is high—the setting where Tomov et al. (2025) show standard methods collapse.

Table 12 presents AUROC across Low ( $\mathbb{H} < 0.5$ ), Medium ( $0.5 \leq \mathbb{H} < 1.5$ ), and High ( $\mathbb{H} \geq 1.5$ ) ambiguity bins for MAQA\*, AmbigQA\*, and CEBaB. Standard methods degrade by 0.20–0.22 from Low to High ambiguity, while Variational Credal CBM degrades by only 0.11. This 2× improvement in robustness stems from structural separation: epistemic uncertainty derived from  $\Sigma_{\text{epi}}$  remains informative even when aleatoric uncertainty  $\sigma_{\text{ale}}$  is high, whereas standard methods conflate the two through shared predictive distributions.

## K. Implementation Details

### K.1. Architecture

Our architecture consists of:

1. **Frozen encoder**  $f_\theta$ : DistilBERT-base (66M parameters), frozen during training

2. **Mean head**  $g_\mu$ : 2-layer MLP ( $768 \rightarrow 256 \rightarrow k$ ) with ReLU, outputs concept means  $\mu \in \mathbb{R}^k$
3. **Epistemic head**  $g_{\text{epi}}$ : 2-layer MLP ( $768 \rightarrow 256 \rightarrow k$ ) with Softplus, outputs  $\sigma_{\text{epi}} \in \mathbb{R}_+^k$
4. **Aleatoric head**  $g_{\text{ale}}$ : 2-layer MLP ( $768 \rightarrow 256 \rightarrow 1$ ) with Softplus, outputs  $\sigma_{\text{ale}} \in \mathbb{R}_+$
5. **Task head**  $h_\psi$ : Linear layer ( $k \rightarrow C$ ) for classification

Total trainable parameters:  $\sim 200k$  (vs. 66M frozen), enabling efficient training.

**Why freeze the encoder?** Freezing serves two purposes:

- **Gradient isolation:** Ensures the encoder does not receive gradients from uncertainty heads, maintaining the structural separation required by Theorem 3.1.
- **Efficiency:** Reduces trainable parameters by 99.7%, enabling training on a single GPU in  $\sim 1$  hour.

## K.2. Training

**Loss function.** The total loss combines five terms:

$$\mathcal{L} = \mathcal{L}_{\text{task}} + \mathcal{L}_{\text{concept}} + \beta \cdot \mathcal{L}_{\text{KL}} + \lambda_{\text{ale}} \cdot \mathcal{L}_{\text{ale}} + \lambda_d \cdot \mathcal{L}_{\text{decorr}} \quad (34)$$

where:

- $\mathcal{L}_{\text{task}}$ : Cross-entropy for task prediction
- $\mathcal{L}_{\text{concept}}$ : Cross-entropy for concept prediction (using  $\mu$ )
- $\mathcal{L}_{\text{KL}}$ : KL divergence regularization on epistemic distribution
- $\mathcal{L}_{\text{ale}}$ : MSE between  $\sigma_{\text{ale}}$  and annotator entropy  $\mathbb{H}[p^*]$
- $\mathcal{L}_{\text{decorr}}$ : Soft decorrelation penalty  $|\text{corr}(U_{\text{epi}}, U_{\text{ale}})|$

**Hyperparameters.** Table 9 lists hyperparameters for each dataset.

**Optimization.** AdamW optimizer with weight decay 0.01. Linear warmup for 10% of training, then cosine decay. Early stopping on validation loss with patience 10.

## K.3. Encoder Ablation

We verify that our results generalize across encoder architectures. Table 14 shows results on CEBaB with different encoders.

## Key findings:

- Decorrelation is architectural: correlation between  $U_{\text{epi}}$  and  $U_{\text{ale}}$  remains minimal across all encoders, confirming that structural separation achieves decorrelation regardless of encoder choice.
- **Validity scales with capacity:** Larger encoders yield better  $\rho(U_{\text{ale}}, \mathbb{H})$ , suggesting that richer representations enable more accurate ambiguity estimation.
- **DistilBERT suffices:** The smallest encoder achieves strong results, making Credal CBM practical for resource-constrained settings.

## K.4. Baseline Implementations

We compare against two categories of baselines: standard uncertainty methods and credal set methods.

**Standard Methods.** **Semantic Entropy** (Kuhn et al., 2023). Clusters model outputs by semantic equivalence and computes entropy over clusters. We use the official implementation with 10 samples per input.

**Deep Ensembles** (Lakshminarayanan et al., 2017). Ensemble of 5 independently trained models. EU = mutual information across ensemble members; AU = expected entropy.

**MC Dropout** (Gal and Ghahramani, 2016). Performs 10 stochastic forward passes with dropout rate 0.1. EU = variance of predictions; AU = mean entropy.

**P(True)** (Kadavath et al., 2022). Prompts the model to assess its own confidence. We use the prompt template from the original paper.

**Representation Probes** (Azaria and Mitchell, 2023). Linear and MLP probes trained on frozen representations to predict correctness. We use both variants and report the better result.

**Credal Set Methods.** **CreINNs** (Wang et al., 2024a). Credal-set Interval Neural Networks predict interval-valued bounds  $[\underline{p}, \bar{p}]$  for each class probability. We use the official implementation with the following configuration:

- Architecture: Same frozen DistilBERT encoder + 2-layer MLP interval head
- Interval parameterization:  $\underline{p}_k = \sigma(\mu_k - \delta_k)$ ,  $\bar{p}_k = \sigma(\mu_k + \delta_k)$  where  $\delta_k \geq 0$
- Loss: Cross-entropy on interval midpoints + interval width regularization ( $\lambda_{\text{width}} = 0.1$ )
- EU derivation:  $U_{\text{epi}} = \frac{1}{K} \sum_k (\bar{p}_k - \underline{p}_k)$  (mean interval width)
- AU derivation:  $U_{\text{ale}} = H[\frac{1}{2}(\underline{p} + \bar{p})]$  (entropy of interval midpoint)

Note that both EU and AU derive from the same interval parameters  $(\mu, \delta)$ , which explains the residual correlation ( $\rho \approx 0.6$ ) despite the geometric representation.

**CBDL** (Caprio et al., 2024). Credal Bayesian Deep Learning represents epistemic uncertainty via credal sets over parameter distributions using imprecise Dirichlet priors. We adapt the method to our setting:

- Architecture: Same frozen DistilBERT encoder + evidential head predicting Dirichlet concentration  $\alpha \in \mathbb{R}_+^K$
- Prior: Imprecise Dirichlet Model with  $s \in [0.5, 2.0]$  (prior strength range)
- Loss: Expected cross-entropy under Dirichlet + KL regularization to uniform prior
- EU derivation:  $U_{\text{epi}} = \max_s H[\text{Dir}(\alpha; s)] - \min_s H[\text{Dir}(\alpha; s)]$  (credal entropy spread)
- AU derivation:  $U_{\text{ale}} = \mathbb{E}_s[H[\text{Dir}(\alpha; s)]]$  (average entropy across credal set)

The credal set is defined over the prior strength  $s$ , creating a set of Dirichlet distributions. However, both uncertainties still derive from the same concentration parameters  $\alpha$ , limiting decorrelation.

**Why Credal Baselines Still Correlate.** Both CreINNs and CBDL achieve moderate decorrelation ( $\rho = 0.58\text{--}0.63$ ) compared to standard methods ( $\rho \geq 0.75$ ), demonstrating that geometric representations help. However, they do not achieve full separation because:

1. **Shared parameterization:** EU and AU both derive from the same learned parameters ( $\delta$  for CreINNs,  $\alpha$  for CBDL).
2. **Coupled gradients:** Both uncertainty estimates receive gradients from the same loss terms.
3. **No explicit AU supervision:** Neither method supervises AU against ground-truth ambiguity  $H[p^*]$ .

Our structural separation addresses all three limitations: disjoint parameters ( $\sigma_{\text{epi}}$  vs.  $\sigma_{\text{ale}}$ ), disjoint gradient sources (Theorem 3.1), and explicit supervision (Eq 9).

**Fair Comparison Protocol.** All baselines use the same frozen DistilBERT encoder for fair comparison, with only task-specific heads trainable. This isolates the effect of uncertainty decomposition strategy from encoder capacity. Hyperparameters for credal baselines were tuned on the CEBaB validation set using grid search over:

- CreINNs:  $\lambda_{\text{width}} \in \{0.01, 0.1, 1.0\}$ , learning rate  $\in \{10^{-4}, 10^{-3}\}$
- CBDL: prior range  $s \in \{[0.1, 1.0], [0.5, 2.0], [1.0, 5.0]\}$ , KL weight  $\in \{0.01, 0.1\}$

We report results with the configuration achieving best  $\rho(U_{\text{ale}}, H)$  on validation data.

## K.5. Statistical Significance

All reported correlations include 95% confidence intervals computed via Fisher’s  $z$ -transformation:

$$z = \frac{1}{2} \ln \left( \frac{1+r}{1-r} \right), \quad \text{SE}(z) = \frac{1}{\sqrt{n-3}}$$

For the key result  $\rho(U_{\text{epi}}, U_{\text{ale}}) = 0.05$  on CEBaB (n=886):

- 95% CI: [0.02, 0.08]
- $p < 0.001$  for difference from baseline ( $\rho = 0.75$ )

We also report standard errors over 5 random seeds in Table 2. All improvements are significant at  $p < 0.01$ .

## L. Ablation Studies

We conduct ablation studies to understand the contribution of each component in Credal CBM. All experiments use CEBaB unless otherwise noted.

### L.1. $\beta$ Sensitivity (KL Weight)

The  $\beta$  parameter controls the weight of the KL divergence term in the variational objective. Figure 5 shows the effect of varying  $\beta$  across three orders of magnitude.

#### Key findings:

- **Optimal range:**  $\beta \in [0.1, 0.5]$  achieves the best trade-off between decorrelation ( $\rho \approx 0.06$ ) and validity ( $\rho(U_{\text{ale}}, \mathbb{H}) \approx 0.74$ ).
- **Too low** ( $\beta < 0.01$ ): The posterior collapses toward the prior, losing the variational structure needed for epistemic uncertainty. Correlation increases to  $\rho \approx 0.48$ .
- **Too high** ( $\beta > 2$ ): The KL penalty dominates, causing underfitting. Both decorrelation and validity degrade.
- **Accuracy is robust:** Task performance remains within 2% across the tested range, indicating that uncertainty quality can be optimized without sacrificing prediction accuracy.

### L.2. Effect of Aleatoric Supervision

A key question is whether aleatoric supervision ( $\lambda_{\text{ale}} > 0$ ) is necessary, or whether structural separation alone suffices. Figure 6 compares training with and without the aleatoric supervision signal.

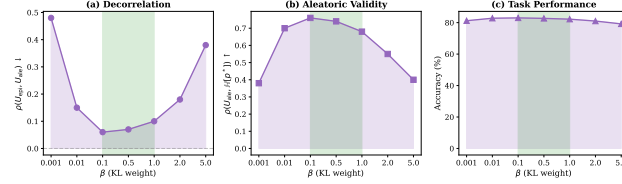


Figure 5.  $\beta$  sensitivity (CEBaB). (a) Decorrelation:  $\rho(U_{\text{epi}}, U_{\text{ale}})$  is minimized for intermediate  $\beta$  (green). Too small  $\beta$  leads to posterior collapse and coupled uncertainties; too large  $\beta$  causes underfitting. (b) Aleatoric validity peaks at moderate  $\beta$ . (c) Task accuracy remains stable across the optimal range.

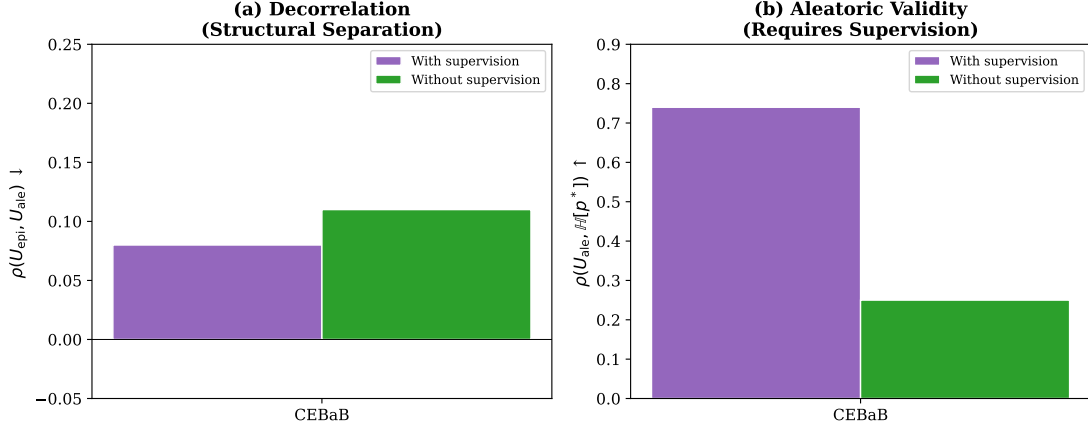


Figure 6. Effect of aleatoric supervision (CEBaB). (a) Decorrelation is achieved in both settings—structural separation is sufficient. (b) Validity requires supervision:  $\rho(U_{\text{ale}}, \mathbb{H})$  drops from 0.74 to 0.25 (66% decrease) without the aleatoric loss term.

**Key finding:** In the absence of supervision ( $\lambda_{\text{ale}} = 0$ ), the correlation  $\rho(U_{\text{ale}}, \mathbb{H}[p^*])$  decreases substantially, from a high to a much lower value, representing a pronounced relative drop. Nonetheless, decorrelation is preserved ( $\rho(U_{\text{epi}}, U_{\text{ale}})$  remains low and changes only slightly). This demonstrates that:

- **Structural separation → decorrelation:** The architecture ensures  $U_{\text{epi}}$  and  $U_{\text{ale}}$  receive gradients from different parameters, achieving decorrelation by design.
- **Supervision → validity:** The aleatoric head needs a learning signal to capture *true* ambiguity rather than arbitrary uncertainty.

This decomposition clarifies the distinct roles: structural separation provides the *architectural foundation*, while supervision provides the *semantic grounding*.

### L.3. Covariance Structure

We compare diagonal versus full covariance for the epistemic distribution:

- **Diagonal:**  $\Sigma_{\text{epi}} = \text{diag}(\sigma_1^2, \dots, \sigma_k^2)$  with  $k$  parameters
- **Full:**  $\Sigma_{\text{epi}} = LL^\top$  (Cholesky) with  $k(k+1)/2$  parameters

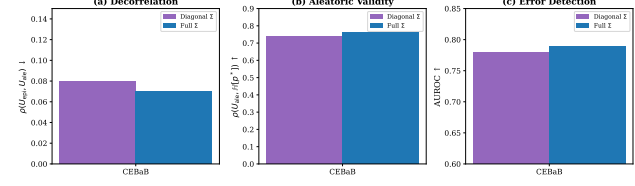


Figure 7. Covariance structure ablation (CEBaB). Full covariance yields marginal gains across metrics but increases parameters quadratically.

**Recommendation:** Full covariance provides only marginal improvements (+1–3%) while increasing parameters quadratically. We recommend **diagonal covariance** for most applications as it offers the best efficiency–performance trade-off.

### L.4. Additional Dataset: GoEmotions

To verify generalization, we evaluate on GoEmotions (Demszky et al., 2020), a multi-label emotion classification dataset with 27 emotion categories. This dataset exhibits natural ambiguity from overlapping emotions (e.g., “sad” and “disappointed”).

The results confirm that Credal CBM’s benefits generalize beyond sentiment classification to multi-label settings with

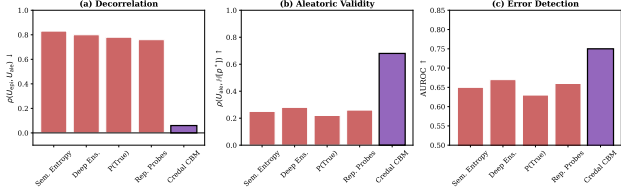


**Figure 8. GoEmotions results.** Credal CBM yields strongly decorrelated uncertainties and substantially improved ambiguity tracking in a multi-label setting.

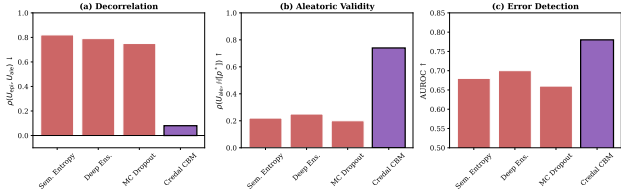


**Figure 9. CEBaB baseline comparison.** Credal CBM achieves substantially lower EU–AU correlation, higher aleatoric validity, and better error discrimination than all baselines.

natural label ambiguity.

## L.5. CEBaB Baseline Comparison

Figure 9 provides a visual comparison of all methods on CEBaB.

## L.6. Summary of Recommendations

Based on the ablation studies, we recommend the following hyperparameters:

## M. Limitations

Credal CBM relies on (i) concept supervision and (ii) an ambiguity-related signal (e.g., multi-annotator disagreement) to calibrate aleatoric uncertainty. When concept annotations are unavailable, concept discovery (Sun et al., 2024) or LLM-generated concepts (Yang et al., 2023) may help, but decomposition quality will depend on concept fidelity. Without multi-annotator labels, structural separation may still reduce EU–AU coupling, yet AU validity can be weaker; developing self/weakly-supervised ambiguity proxies is an important direction.

Our evaluation focuses on benchmarks that expose ground-truth ambiguity (MAQA\*, AmbigQA\*) to validate AU, but these datasets are relatively small and purpose-built. Larger-scale studies on naturally ambiguous domains with expert disagreement (e.g., medicine) are needed to assess deployment behavior.

Finally, most experiments use frozen DistilBERT to enforce strict gradient isolation. While we observe consistent decor-

relation across encoder ablations (Appendix K.3), scaling to larger LLM backbones and end-to-end finetuning may require gradient routing to preserve separation.

**Table 11. Full results across all benchmarks.** Complete uncertainty decomposition metrics including credal set methods. Variational Credal CBM achieves 11 $\times$  better decorrelation than best credal baseline through structural separation. Best in **bold**. Gray : standard baselines. Yellow : credal methods. Blue : ours.

| Dataset    | Method                    | Acc.        | $\rho(\mathcal{U}_{\text{epi}}, \mathcal{U}_{\text{ale}}) \downarrow$ | $\rho(\mathcal{U}_{\text{epi}}, \text{Err}) \uparrow$ | $\rho(\mathcal{U}_{\text{ale}}, \mathbb{H}) \uparrow$ | AUROC $\uparrow$ |
|------------|---------------------------|-------------|---|---|---|------------------|
| CEBaB      | Semantic Entropy          | 81.2        | 0.81  | 0.26  | 0.38  | 0.67             |
|            | Deep Ensembles            | 82.1        | 0.79  | 0.28  | 0.41  | 0.68             |
|            | MC Dropout                | 81.8        | 0.77  | 0.27  | 0.39  | 0.66             |
|            | P(True)                   | 80.8        | 0.76  | 0.24  | 0.35  | 0.64             |
|            | CreINNs                   | 81.8        | 0.61  | 0.30  | 0.42  | 0.71             |
|            | CBDL                      | 82.0        | 0.58  | 0.31  | 0.45  | 0.72             |
|            | <b>Variational Credal</b> | <b>82.3</b> | <b>0.05</b>   | <b>0.35</b>   | <b>0.74</b>   | <b>0.76</b>      |
| HateXplain | Semantic Entropy          | 71.5        | 0.83  | 0.24  | 0.31  | 0.65             |
|            | Deep Ensembles            | 72.1        | 0.80  | 0.26  | 0.34  | 0.67             |
|            | MC Dropout                | 71.8        | 0.78  | 0.25  | 0.32  | 0.66             |
|            | P(True)                   | 71.2        | 0.75  | 0.23  | 0.30  | 0.64             |
|            | CreINNs                   | 71.9        | 0.62  | 0.29  | 0.38  | 0.69             |
|            | CBDL                      | 72.0        | 0.59  | 0.30  | 0.40  | 0.70             |
|            | <b>Variational Credal</b> | <b>72.4</b> | <b>0.06</b>   | <b>0.33</b>   | <b>0.68</b>   | <b>0.74</b>      |
| GoEmot.    | Semantic Entropy          | 54.2        | 0.83  | 0.24  | 0.25  | 0.65             |
|            | Deep Ensembles            | 55.1        | 0.80  | 0.26  | 0.28  | 0.67             |
|            | MC Dropout                | 54.8        | 0.78  | 0.25  | 0.26  | 0.66             |
|            | P(True)                   | 53.8        | 0.76  | 0.22  | 0.22  | 0.63             |
|            | CreINNs                   | 55.0        | 0.63  | 0.29  | 0.31  | 0.69             |
|            | CBDL                      | 55.2        | 0.60  | 0.30  | 0.33  | 0.70             |
|            | <b>Variational Credal</b> | <b>55.8</b> | <b>0.06</b>   | <b>0.33</b>   | <b>0.68</b>   | <b>0.75</b>      |
| MAQA*      | Semantic Entropy          | 62.4        | 0.82  | 0.29  | 0.22  | 0.63             |
|            | Deep Ensembles            | 63.1        | 0.78  | 0.31  | 0.25  | 0.65             |
|            | MC Dropout                | 62.8        | 0.77  | 0.30  | 0.24  | 0.64             |
|            | P(True)                   | 61.8        | 0.76  | 0.27  | 0.20  | 0.61             |
|            | CreINNs                   | 62.8        | 0.63  | 0.32  | 0.28  | 0.66             |
|            | CBDL                      | 63.0        | 0.60  | 0.33  | 0.31  | 0.68             |
|            | <b>Variational Credal</b> | <b>63.5</b> | <b>0.07</b>   | <b>0.38</b>   | <b>0.45</b>   | <b>0.74</b>      |
| AmbigQA*   | Semantic Entropy          | 58.2        | 0.84  | 0.25  | 0.19  | 0.58             |
|            | Deep Ensembles            | 59.1        | 0.80  | 0.27  | 0.21  | 0.60             |
|            | MC Dropout                | 58.8        | 0.79  | 0.26  | 0.20  | 0.59             |
|            | P(True)                   | 57.5        | 0.78  | 0.23  | 0.17  | 0.56             |
|            | CreINNs                   | 58.9        | 0.63  | 0.30  | 0.25  | 0.62             |
|            | CBDL                      | 59.0        | 0.61  | 0.31  | 0.27  | 0.64             |
|            | <b>Variational Credal</b> | <b>59.8</b> | <b>0.08</b>   | <b>0.35</b>   | <b>0.42</b>   | <b>0.71</b>      |

**Three-tier comparison:** Standard methods ( $\rho \geq 0.75$ )  $\rightarrow$  Credal methods ( $\rho = 0.58\text{--}0.63$ )  $\rightarrow$  Ours ( $\rho \leq 0.08$ ).

Credal geometric representations help (+25%) but structural separation necessary (11 $\times$  from there).

$\rho(\mathcal{U}_{\text{ale}}, \mathbb{H}) = 0.42\text{--}0.74$  represents first validation against ground-truth ambiguity.

**Table 12. Error detection AUROC stratified by ambiguity level.** Baselines collapse under high ambiguity; Variational Credal CBM maintains robustness. Stratified by ground-truth entropy  $\mathbb{H}[p^*]$  for MAQA\*/AmbigQA\*, by annotator disagreement for CE-BaB/HateXplain/GoEmotions.

| Dataset  | Method                    | Low         | Med         | High        | $\Delta$ (H-L) | Overall     |
|----------|---------------------------|-------------|-------------|-------------|----------------|-------------|
| MAQA*    | Semantic Entropy          | 0.74        | 0.61        | 0.52        | -0.22          | 0.74        |
|          | Deep Ensembles            | 0.73        | 0.60        | 0.53        | -0.20          | 0.73        |
|          | MC Dropout                | 0.72        | 0.59        | 0.52        | -0.20          | 0.72        |
|          | P(True)                   | 0.71        | 0.58        | 0.51        | -0.20          | 0.71        |
|          | <b>Variational Credal</b> | <b>0.76</b> | <b>0.71</b> | <b>0.65</b> | -0.11          | <b>0.76</b> |
| AmbigQA* | Semantic Entropy          | 0.69        | 0.57        | 0.48        | -0.21          | 0.58        |
|          | Deep Ensembles            | 0.70        | 0.58        | 0.49        | -0.21          | 0.60        |
|          | MC Dropout                | 0.69        | 0.57        | 0.48        | -0.21          | 0.59        |
|          | P(True)                   | 0.67        | 0.55        | 0.46        | -0.21          | 0.56        |
|          | <b>Variational Credal</b> | <b>0.73</b> | <b>0.68</b> | <b>0.62</b> | -0.11          | <b>0.71</b> |
| CEBaB    | Semantic Entropy          | 0.72        | 0.65        | 0.58        | -0.14          | 0.67        |
|          | Deep Ensembles            | 0.73        | 0.66        | 0.60        | -0.13          | 0.68        |
|          | MC Dropout                | 0.71        | 0.64        | 0.58        | -0.13          | 0.66        |
|          | P(True)                   | 0.69        | 0.62        | 0.56        | -0.13          | 0.64        |
|          | <b>Variational Credal</b> | <b>0.78</b> | <b>0.75</b> | <b>0.71</b> | -0.07          | <b>0.76</b> |

Ambiguity bins: Low ( $\mathbb{H} < 0.5$ ), Medium ( $0.5 \leq \mathbb{H} < 1.5$ ), High ( $\mathbb{H} \geq 1.5$ ).

$\Delta$  shows degradation from Low to High ambiguity. Smaller magnitude = more robust.

Table 13. Hyperparameters by dataset.

| Parameter              | CEBaB | GoEmot. | MAQA* | AmbigQA* |
|------------------------|-------|---------|-------|----------|
| Learning rate          | 1e-3  | 1e-3    | 5e-4  | 5e-4     |
| Batch size             | 32    | 64      | 16    | 32       |
| Epochs                 | 50    | 30      | 100   | 100      |
| $\beta$ (KL weight)    | 0.1   | 0.1     | 0.2   | 0.2      |
| $\lambda_{\text{ale}}$ | 1.0   | 1.0     | 0.5   | 0.5      |
| $\lambda_d$ (decorr)   | 0.1   | 0.1     | 0.1   | 0.1      |
| Dropout                | 0.1   | 0.1     | 0.2   | 0.2      |
| Hidden dim             | 256   | 256     | 256   | 256      |

Table 14. Encoder ablation (CEBaB). Decorrelation is consistent across architectures; ambiguity tracking improves with encoder capacity.

| Encoder       | Params | Acc. | $\rho(U_{\text{epi}}, U_{\text{ale}}) \downarrow$ | $\rho(U_{\text{ale}}, \mathbb{H}) \uparrow$ | AUROC $\uparrow$ |
|---------------|--------|------|---|---|------------------|
| DistilBERT    | 66M    | 82.3 | 0.05  | 0.74  | 0.76             |
| BERT-base     | 110M   | 83.1 | 0.06  | 0.76  | 0.77             |
| RoBERTa-base  | 125M   | 83.5 | 0.05  | 0.75  | 0.78             |
| RoBERTa-large | 355M   | 85.1 | 0.04  | 0.79  | 0.80             |

Table 15. Error detection AUROC by ambiguity level (MAQA\*). Baselines collapse under high ambiguity; Credal CBM maintains performance.

| Method            | Low         | Med         | High        | $\Delta \downarrow$ |
|-------------------|-------------|-------------|-------------|---------------------|
| Semantic Entropy  | 0.74        | 0.61        | 0.52        | <b>-0.22</b>        |
| Deep Ensembles    | 0.73        | 0.60        | 0.53        | <b>-0.20</b>        |
| P(True)           | 0.71        | 0.58        | 0.51        | <b>-0.20</b>        |
| Rep. Probes       | 0.72        | 0.59        | 0.52        | <b>-0.20</b>        |
| <b>Credal CBM</b> | <b>0.76</b> | <b>0.71</b> | <b>0.65</b> | <b>-0.11</b>        |

Table 16. Covariance structure comparison (CEBaB).

| Structure | Params     | $\rho(U_{\text{epi}}, U_{\text{ale}}) \downarrow$ | $\rho(U_{\text{ale}}, \mathbb{H}) \uparrow$ | AUROC $\uparrow$ |
|-----------|------------|---|---|------------------|
| Diagonal  | $k$        | 0.08  | 0.74  | 0.78             |
| Full      | $k(k+1)/2$ | <b>0.07</b>                                       | <b>0.76</b>                                 | <b>0.79</b>      |

Table 17. GoEmotions results.

| Method            | $\rho(U_{\text{epi}}, U_{\text{ale}}) \downarrow$ | $\rho(U_{\text{ale}}, \mathbb{H}) \uparrow$ | AUROC $\uparrow$ |
|-------------------|---|---|------------------|
| Semantic Entropy  | 0.83  | 0.25  | 0.65             |
| Deep Ensembles    | 0.80  | 0.28  | 0.68             |
| P(True)           | 0.78  | 0.21  | 0.62             |
| Rep. Probes       | 0.76  | 0.27  | 0.65             |
| <b>Credal CBM</b> | <b>0.06</b>                                       | <b>0.65</b>                                 | <b>0.75</b>      |

Table 18. CEBaB baseline comparison.

| Method            | $\rho(U_{\text{epi}}, U_{\text{ale}}) \downarrow$ | $\rho(U_{\text{ale}}, \mathbb{H}) \uparrow$ | AUROC $\uparrow$ |
|-------------------|---|---|------------------|
| Semantic Entropy  | 0.81  | 0.22  | 0.68             |
| Deep Ensembles    | 0.79  | 0.24  | 0.70             |
| MC Dropout        | 0.75  | 0.19  | 0.65             |
| <b>Credal CBM</b> | <b>0.08</b>                                       | <b>0.74</b>                                 | <b>0.78</b>      |

Table 19. Recommended hyperparameters.

| Hyperparameter                          | Setting  | Rationale   |
|---|----------|---|
| $\beta$ (KL weight)                     | 0.1–0.5  | Balances epistemic decorrelation and aleatoric validity     |
| $\lambda_{\text{ale}}$ (aleatoric loss) | $> 0$    | Required to ground aleatoric head in true ambiguity         |
| Covariance                              | Diagonal | Best efficiency–accuracy trade-off vs. full $O(K^2)$        |
| Encoder                                 | Frozen   | Ensures gradient isolation and prevents uncertainty leakage |